The Abdus Salam
International Centre for Theoretical Physics

United Nations
Educational, Scientific
and Cultural Organization

International Atomic
Energy Agency

H4.SMR/1645-24

"2nd Workshop on Earthquake Engineering for Nuclear Facilities: Uncertainties in Seismic Hazard"

14 - 25 February 2005

# Case Study: Modern SHA on performance based earthquake engineering

*Fabio Romanelli*

Dept. of Earth Sciences
Trieste

Strada Costiera 11, 34014 Trieste, Italy - Tel. +39 040 2240 111; Fax +39 040 224 163 - sci_info@ictp.it, www.ictp.it

2nd Workshop on Earthquake Engineering for Nuclear Facilities. Uncertainties in Seismic Hazard Assessment
Miramar, 2005

# Case Study: Modern SHA on performance based earthquake engineering

Fabio ROMANELLI
Dept. Earth Sciences
Università degli studi di Trieste
romanel@dst.units.it

# Outline

- **SHA introductory remarks**
  - SHA & PBDE
  - Site & source effects
  - Definition of seismic input
  - Demand parameters
- **Realistic definition of seismic input**
  - Parametric studies
    - Focal mechanism
    - Site effects
    - Directivity
- **Conclusions**

# SHA Dualism

Deterministic vs. probabilistic approaches to assessing earthquake hazards and risks have differences, advantages, and disadvantages that often make the use of one advantageous over the other.

Probabilistic methods can be viewed inclusive of all deterministic events with a finite probability of occurrence. In this context, proper deterministic methods that focus on a single earthquake ensure that that event is realistic, i.e. that it has a finite probability of occurrence.

**Determinism vs. probabilism is not a bivariate choice but a continuum in which both analyses are conducted, but more emphasis is given to one over the other. Emphasis here means weight in the decision-making process, regarding**

Modified from: **Mc Guire, 2001**



# SH assessment

| | Deterministic | | | Probabilistic |
|---|---|---|---|---|
| **Risk mitigation decision** | Emergency response | | | Design/Retrofit |
| **Seismic environment** | Next to active fault | High hazard, plate margin | Moderate hazard, anywhere | Low hazard, midplate |
| **Scope of the project** | Regional risk | | Multiple properties lifelines | Specific site |
| | **Qualitative** | | | **Quantitative** |

Modified from: **Mc Guire, 2001**

PSHA

In many applications a **recursive analysis**, where deterministic interpretations are triggered by probabilistic results and vice versa, will give the greatest insight and allow the most informed decisions to be made.

PEER Report

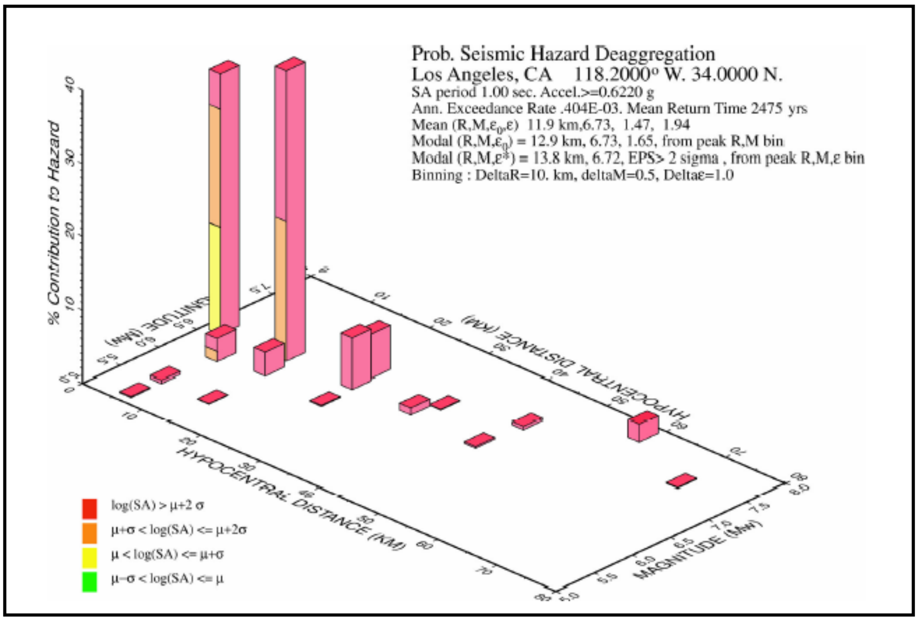




# Estimation of Ground Motion

PSHA

| PSHA | Waveform modelling |
|---|---|
| Accounts for all potentially damaging earthquakes in a region | Focus on selected controlling earthquakes |
| Single parameter | Complete time series |
| Deeply rooted in engineering practice (e.g. building codes) | Dynamic analyses of critical facilities |

Disaggregation, recursive analysis ⇨ ⇦ Study of attenuation relationships

## SITE EFFECTS

**Surface topography effects** (convexity)

sensitivity to:

a) type of wavefield

b) angle of incidence

c) shape and sharpness

**Soft surface layering**

a) 1-D: trapping of waves for impedance contrast

(vertical resonances)

$f_n=(2n+1)\beta/4H$

$A \approx (\rho 2\ v2)/(\rho 1\ v1)$

b) 2-D 3-D: complex energy focusing

for diffraction effects

(basin edge waves)



## Empirical techniques for Site effect estimation

**Weak (and strong) motion**

a) S/B spectral ratio
(Borcherdt, 1970)

b) generalized inversion scheme
(Andrews, 1986)

c) coda waves analysis
(Margheriti et al., 1994)

d) parametrized source and path inversion
(Boatwright et al., 1991)

e) H/V spectral ratio (receiver function)
(Lermo et al., 1993)

$$R_{ij}(\omega) = So_i(\omega) \cdot P_{ij}(\omega) \cdot S_j(\omega)$$

**Microtremors**

a) peak frequencies examination

b) S/B spectral ratio

c) H/V spectral ratio
(Nagoshi, 1971; Nakamura, 1989)

d) array analysis
(Malagnini et al., 1993)

# Important issues in SRE

- **Near surface effects**: impedance contrast, velocity
  - geological maps, $v_{30}$, $v_{1/4}$, ??
- **Basin effects**
  - Basin-edge induced waves
  - Subsurface focusing

Modified from: Field et al., 2000



# SRE and SHA

Amplification patterns may vary greatly among the earthquake scenarios, considering different **source locations** (and rupture ...)

SCEC Phase 3 Report

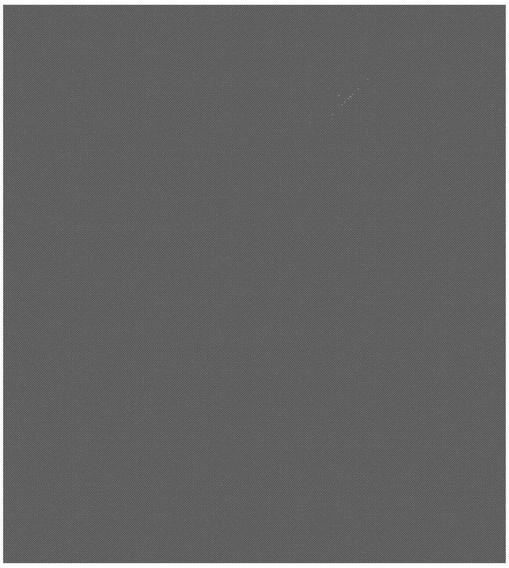

The convolutional model is ultimately artificial (e.g. fault rupturing along the edge of a deep basin)

# SRE and PSHA

- In PSHA the site effect should be defined as the **average behavior**, relative to other sites, given **all** potentially damaging earthquakes
- This produces an intrinsic variability with respect to different earthquake locations, that cannot exceed the difference between sites
- Site characterization:
  - which velocity?
  - use of basin depth effect? Is it a proxy for backazimuth distance?
  - how to reduce aleatoric uncertainty?



# Demand parameters

## DAMAGE POTENTIAL OF EARTHQUAKE GROUND MOTION

**A demand parameter is defined as a quantity that relates seismic input (ground motion) to structural response**

Damage depends on intensity of the various earthquake hazard parameters: ground motion accelerations levels, frequency content of the waves arriving at the site, duration of strong ground motion, etc.

Damage also depends on the earthquake resistance characteristics of the structure, such as its lateral force-resisting system, dynamic properties, dissipation capacity, etc.

# PGA…

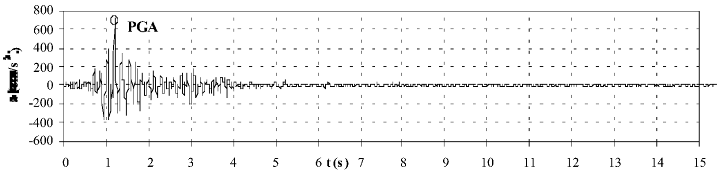


Figure 1 – Acceleration time history. Rocca NS record. 1971 Ancona earthquake ($M_L$=4.7)

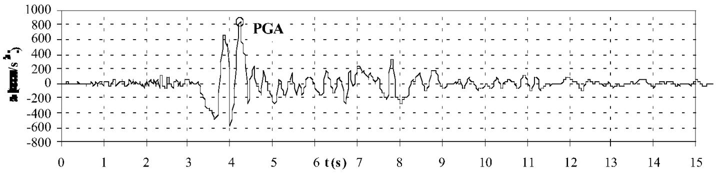


Figure 2 – Acceleration time history. Sylmar N360 record. 1994 Northridge earthquake ($M_w$=6.7)

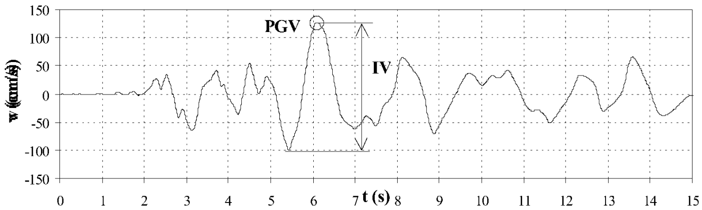


Figure 3 – Velocity time history. Takatori 000 record. 1995 Kobe earthquake ($M_w$=6.9)



# EPA

The effective peak acceleration EPA is defined as the average spectral acceleration over the period range 0.1 to 0.5 s divided by 2.5 (the standard amplification factor for a 5% damping spectrum), as follows:

$$EPA = \frac{\overline{S}_{pa}}{2.5}$$

where $\overline{S}_{pa}$ is mean pseudo-acceleration value. The empirical constant 2.5 is essentially an amplification factor of the response spectrum obtained from real peak value records.

EPA is correlated with the real peak value, but not equal to nor even proportional to it. If the ground motion consists of high f requency components, EPA will be obviously smaller than the real peak value.

It represents the acceleration which is most closely rel ated to the structural response and to the damage potential of an earthquake. The EPA values for the two records of Ancona and Sylmar stations a re 205 cm/s$^2$ and 774 cm/s$^2$ respectively, and describe in a more appropriate way, than PGA values, the damage caused by the two earthquakes.

## Yielding resistance

Linear elastic response spectra recommended by seismic codes have been proved to be inadequate by recent seismic events, as they are not directly related to structural damage. Extremely important factors such as the duration of the strong ground motion and the sequence of acceleration pulses are not taken into account adequately.

Therefore response parameters based on the inelastic behaviour of a structure should be considered with the ground motion characteristics.

In current seismic regulations, the displacement ductility ratio $\mu$ is generally used to reduce the elastic design forces to a level which implicitly considers the possibility that a certain degree of inelastic deformations could occur. To this purpose, employing numerical methods, constant ductility response spectra were derived through non-linear dynamic analyses of viscously damped SDOF systems by defining the following two parameters:

$$C_y = \frac{R_y}{mg} \quad \eta = \frac{R_y}{m\ddot{u}_{g(\max)}} = \frac{C_y}{\ddot{u}_{g(\max)}/g}$$

where $R_y$ is the yielding resistance, m is the mass of the system, and $\ddot{u}_{g(\max)}$ is the maximum ground acceleration.



$$C_y = \frac{R_y}{mg} \qquad (R_y = \text{yielding strength})$$

$$\eta = \frac{R_y}{m\ddot{u}_{g(\max)}} = \frac{C_y}{\ddot{u}_{g(\max)}/g}$$

$$\mu = \frac{u_{max}}{u_y}$$

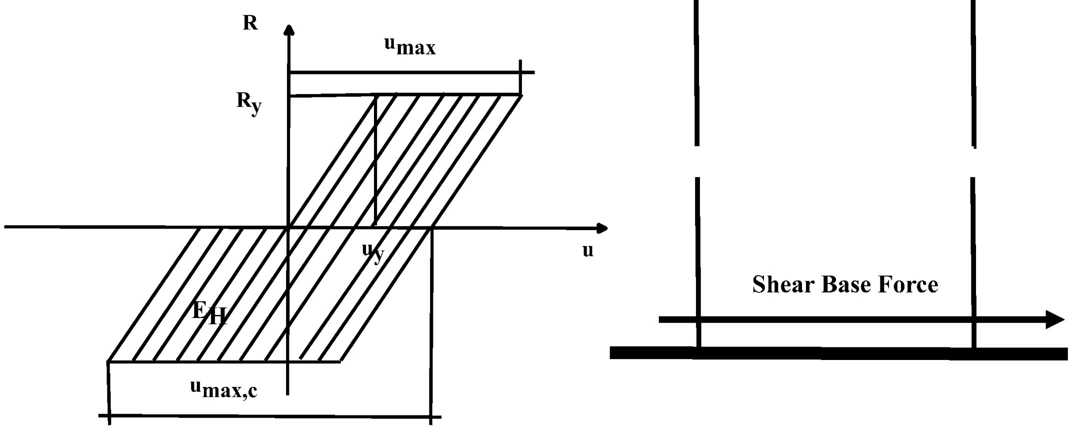

# Yielding resistance 2

The parameter $C_y$ represents the structure's yielding seismic resistance coefficient and $\eta$ expresses a system's yield strength relative to the maximum inertia force of an infinitely rigid system and reveals the strength of the system as a fraction of its weight relative to the peak ground acceleration expressed as a fraction of gravity. Traditionally, displacement ductility was used as the main parameter to measure the degree of damage sustained by a structure.

One significant disadvantage of seismic resistance ($C_y$) spectra is that the effect of strong motion duration is not considered. An example of constant ductility $C_y$ spectra, corresponding to the 1986 San Salvador earthquake (CIG record) and 1985 Chile earthquake (Llolleo record): it seems that the damage potential of these ground motions is quite similar, even though the CIG and Llolleo are records of two earthquakes with very different magnitude, 5.4 and 7.8, respectively.

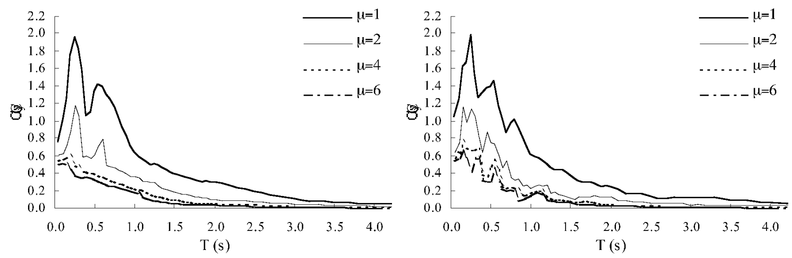


(a) (b)



# Input energy

Introduction of appropriate parameters defined in terms of energy can lead to more reliable estimates, since, more than others, the concept of energy provides tools which allow to account rationally for the mechanisms of generation, transmission and destructiveness of seismic actions.

Energy-based parameters, allowing us to characterize properly the different types of time histories (impulsive, periodic with long durations pulses, etc.) which may correspond to an earthquake, could provide more insight into the seismic performance.

The most promising is the Earthquake Input Energy ($E_I$) and associate parameters (the damping energy $E_\xi$ and the plastic hysteretic energy $E_H$) introduced by Uang & Bertero (1990). This parameter considers the inelastic behavior of a structural system and depends on the dynamic features of both the strong motion and the structure.

The formulation of the energy parameters derives from the following balance energy equation (Uang & Bertero, 1990):

$$E_I = E_k + E_\xi + E_s + E_H$$

where ($E_I$) is the input energy, ($E_k$) is the kinetic energy, ($E_\xi$) is the damping energy, ($E_s$) is the elastic strain energy, and ($E_H$) is the hysteretic energy.

# Input energy

$E_I$ represents the work done by the total base shear at the foundation displacement. The input energy can be expressed by:

$$\frac{E_I}{m} = \int \ddot{u}_t du_g = \int \ddot{u}_t \dot{u}_g dt$$

where m is the mass, $u_t = u + u_g$ is the absolute displacement of the mass, and $u_g$ is the earthquake ground displacement. Usually the input energy per unit mass, i.e. $E_I/m$, is simply denoted as $E_I$.

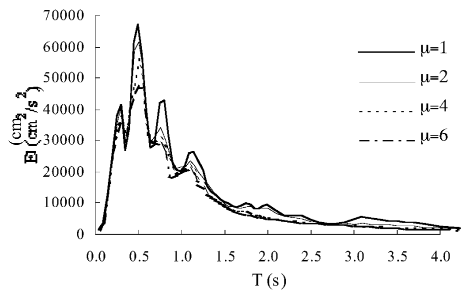


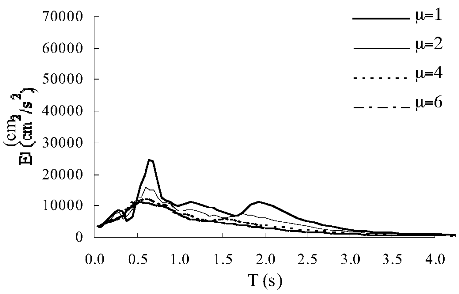


(a) (b)

Comparison between constant ductility input energy $E_I$ spectra. (a) 1986 San Salvador earthquake (CIG record); 1985 Chile earthquake (Llolleo record)



## Landers, 1992

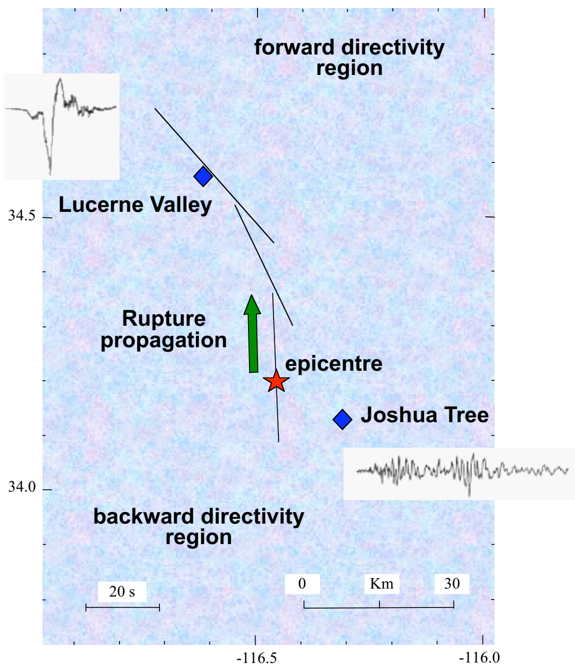


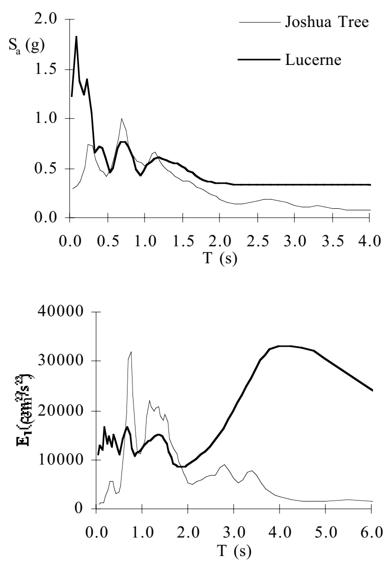

# Know the Input...

A proper definition of the seismic input at a given site can be done following two main approaches:

The first approach is based on the analysis of the available **strong motion databases**, collected by existing seismic networks, and on the grouping of those accelerograms that contain similar source, path and site effects

The second approach is based on **modelling techniques**, developed from the knowledge of the seismic source process and of the propagation of seismic waves, that can realistically simulate the ground motion



# Validation

- The ideal procedure is to follow the two complementary ways, in order to **validate** the numerical modelling with the available recordings.
- Validation and calibration should consider intensity measures (PGA, PGV, PGD, SA, etc.) as well as other characteristics (e.g. duration).
- The misfits can be due to variability in the physical (e.g. point-source) and/or the parameters models adopted.

# Time histories selection

- They are used to extract a measure, representing adequately:
  - Magnitude, distance
  - Source characteristics (fling, directivity)
  - Path effects (attenuation, regional heterogeneities)
  - Site effects (amplification, duration)



# Time histories selection

Ground acceleration, velocity and displacement, recorded at a strong-motion seismometer that was located directly above the part of a fault that ruptured during the 1985 Mw = 8.1, Michoacan, Mexico earthquake.

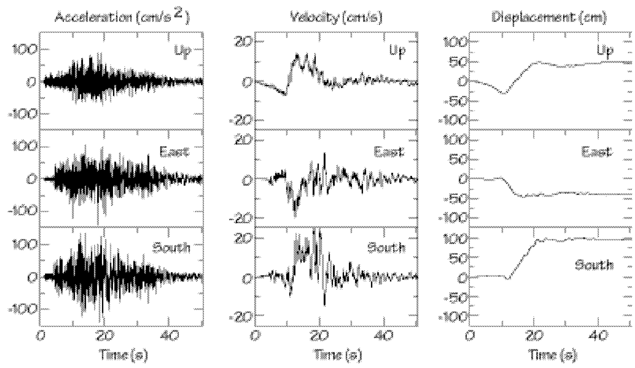


The scenarios have to be based on significant ground motion parameters (e.g. velocity and displacement).

# to bound the output...

- Particularly, in the case of **forward rupture directivity** most of the energy arrives in a single large pulse of motion which may give rise to particularly severe ground motion at sites toward which the fracture propagation progresses.
  - it involves the transmission of large energy amounts to the structures in a very short time.
- These shaking descriptors, strictly linked with energy demands, are relevant (even more than acceleration), especially when dealing with seismic isolation and passive energy dissipation in buildings.



# Some conclusions

While waiting for the enlargement of the strong motion data set, a very useful approach to properly define the seismic input is the development and use of modeling tools based on:
1) the theoretical knowledge of the **physics** of **the seismic source and of wave propagation**;
2) exploitation of the rich **database** about the geotechnical, geological, tectonic, seismotectonic, historical information already available.

**Parametric studies** allow the computation of a wide set of time histories and spectral information, corresponding to possible groundshaking scenarios, for different source models and site conditions.

# References

Mc Guire, R. K. (2001). "Deterministic vs. probabilistic earthquake hazards and risks", **Soil Dynamics and Earthquake Engineering**, 21, 377-384.

Field, E.H., the SCEC Phase III Working Group (2000). "Accounting for site effects in probabilistic seismic hazard analyses of Southern California: overview of the SCEC Phase III report", **Bull. Seism. Soc. Am.**, 90, 6B, p. S1-S31.

Panza, G.F., Romanelli, F. and Vaccari, F. (2001). "Seismic wave propagation in laterally heterogeneous anelastic media: theory and applications to the seismic zonation", **Advances in Geophysics**, Academic press, 43, 1-95.

Panza, G. F., Romanelli, F.,Vaccari, F., Decanini, L. and Mollaioli, F. (2004). "Seismic ground motion modeling and damage earthquake scenarios: possible bridge between seismologists and seismic engineers", **IUGG Special Volume**, Earthquake Hazard, Risk, and Strong Ground Motion (319).

**PEER 2001/09** - Ground Motion Evaluation Procedures for Performance-Based Design, J. Stewart, S. Chiou, J. Bray, R. Graves, P. Somerville, N. Abrahamson

# VAB Project (EC)

ADVANCED METHODS FOR ASSESSING THE SEISMIC VULNERABILITY OF EXISTING MOTORWAY BRIDGES

**ARSENAL RESEARCH**, Vienna, Austria; **ISMES S.P.A**,. Bergamo, Italy; **ICTP**, Trieste, Italy; **UPORTO**, Porto, Portugal; **CIMNE**, Barcelona, Spain; **SETRA**, Bagneaux, France; **JRC-ISPRA**, EU.

Effects on bridge seismic response of asynchronous motion at the base of bridge piers

# Warth bridge

The bridge was designed for a horizontal acceleration of 0,04 g using the quasi static method.

According to the new Austrian seismic code the bridge is situated in zone 4 with a horizontal design acceleration of about 0,1 g: a detailed seismic vulnerability assessment was necessary.

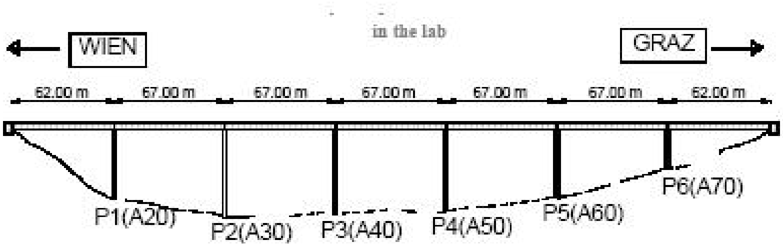


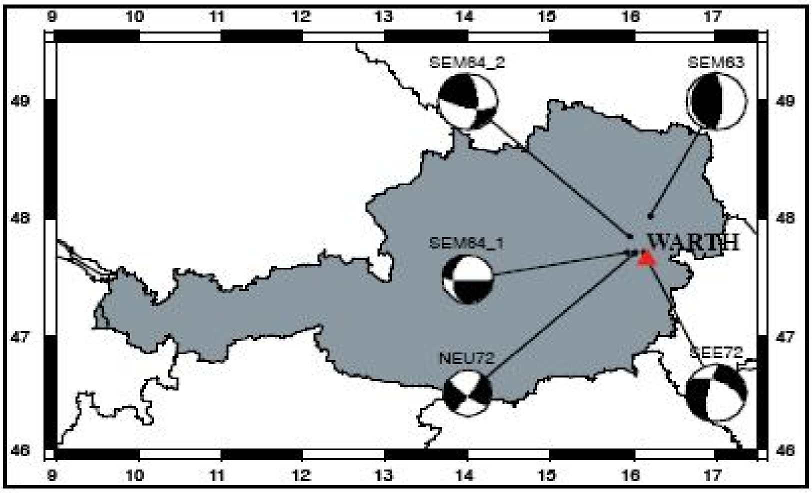


S1
Seebenstein 1972

Strike = 190°
Dip = 70°
Rake = 324°
Depth = 5 km
Mw = 5.5
Distance = 8.7 km

Definition of sources

# Source models

1) **Database of focal mechanism**

| Longitude (°) | Latitude (°) | Focal Depth (km) | Strike (°) | Dip (°) | Rake (°) | Magnitude Ms (Mb) |
|---|---|---|---|---|---|---|
| 16.200 | 48.030 | | 180 | 20 | 90 | |
| 15.920 | 47.730 | 3 | 90 | 81 | 311 | (4.7) |
| 15.950 | 47.850 | 1 | 100 | 70 | 31 | (5.4) |
| 16.120 | 47.730 | 18 | 190 | 70 | 324 | 5.5 (4.9) |
| 16.020 | 47.730 | 19 | 127 | 80 | 190 | 4.4 |

Maximum Historical Earthquake

2) **Parametric study on focal mechanism:**

**strike**
**dip**
**rake**
**depth**

Maximum Credible Earthquake

Maximum Design Earthquake

# Structural models

## STRUCTURAL MODELS

### Bedrock model

1) EUR-I Data set

2) updated on the basis of the geological informations collected by CIMG

### Local LHET model

1) available Warth bridge section plan

2) updated on the basis of the refraction surveys by CIMG

# Initial regional model

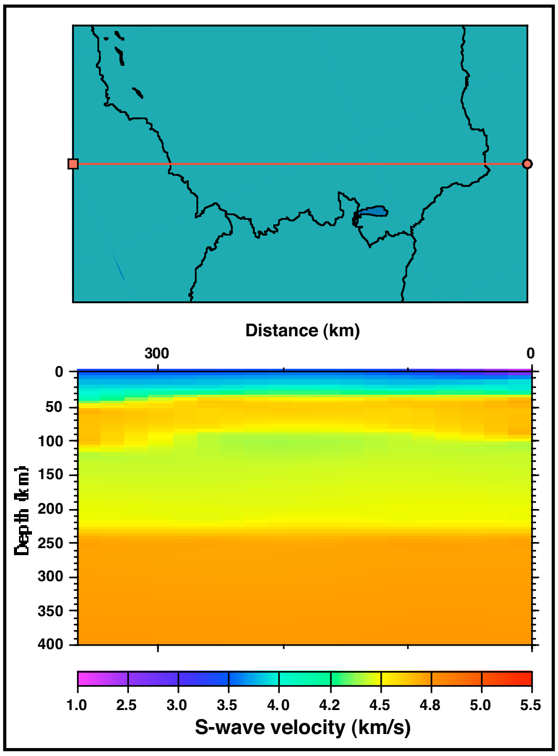


EUR I data set

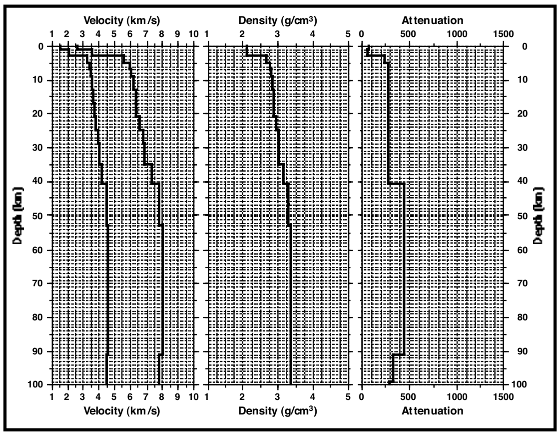


Definition of str. models

# Final bedrock model

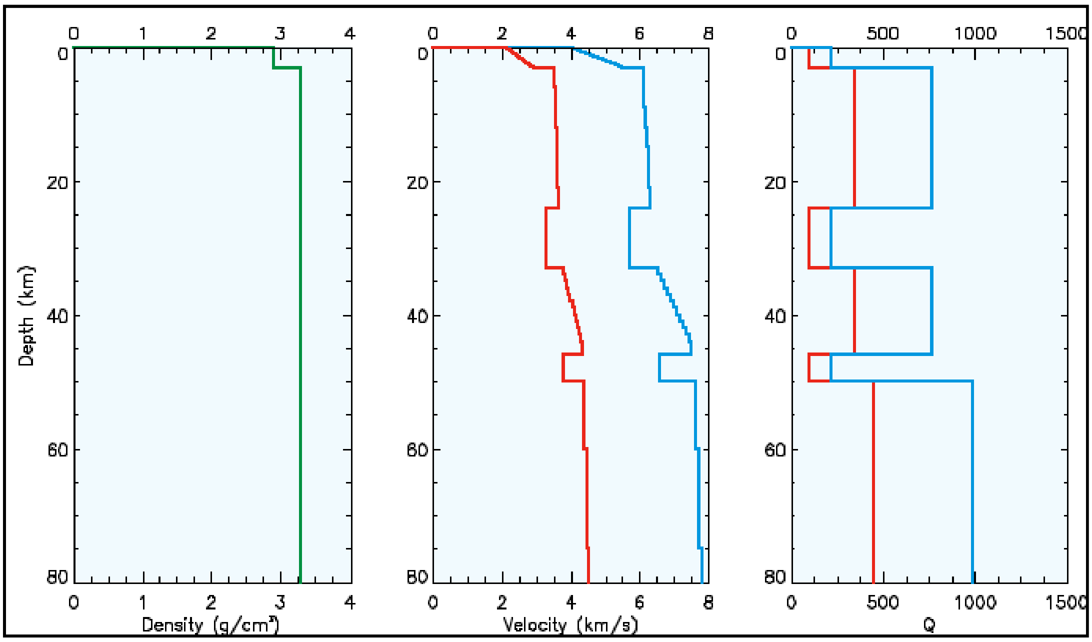


Definition of str. models

# Initial LHM - Warth bridge - model

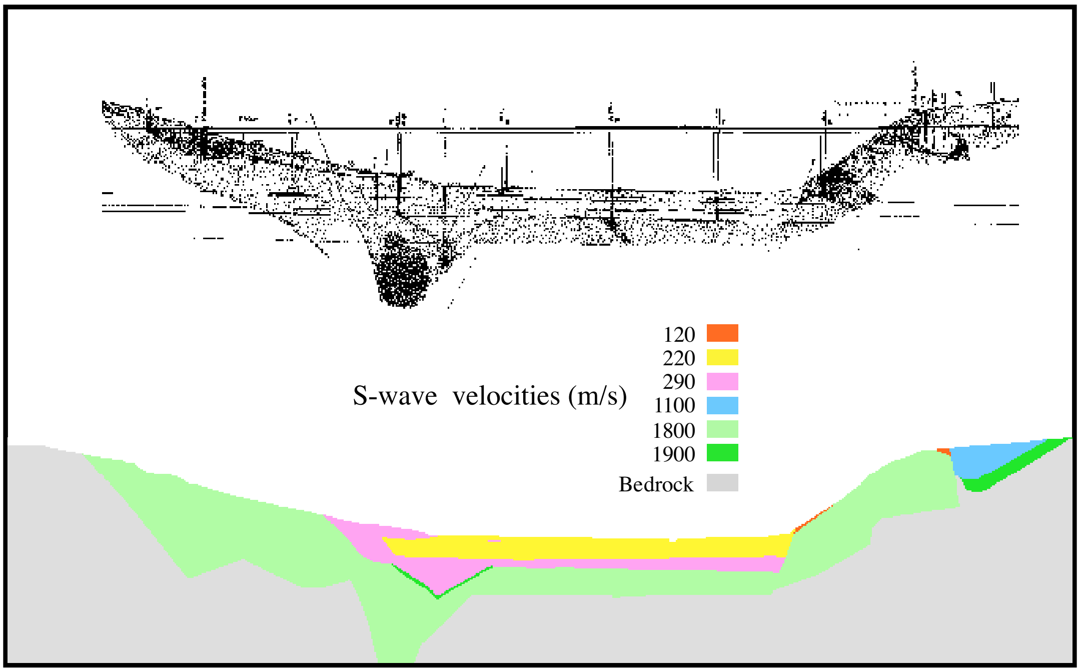


Definition of str. models

# COMPUTATION OF SEISMIC INPUT

PRELIMINARY COMPUTATION

INITIAL source and structural models
3 components of motion
Displacement, velocity, acceleration

FINAL COMPUTATION

FINAL source and structural models
3 components of motion
Displacement, velocity, acceleration

SEISMIC INPUT

1) 1D 10 Hz Parametric study
2) 2D 8Hz

DIFFERENTIAL MOTION

1) time domain
2) spectral domain

SITE RESPONSE

1) Fourier spectral ratios
2) Response spectral ratios

# Hybrid method: MS-FD

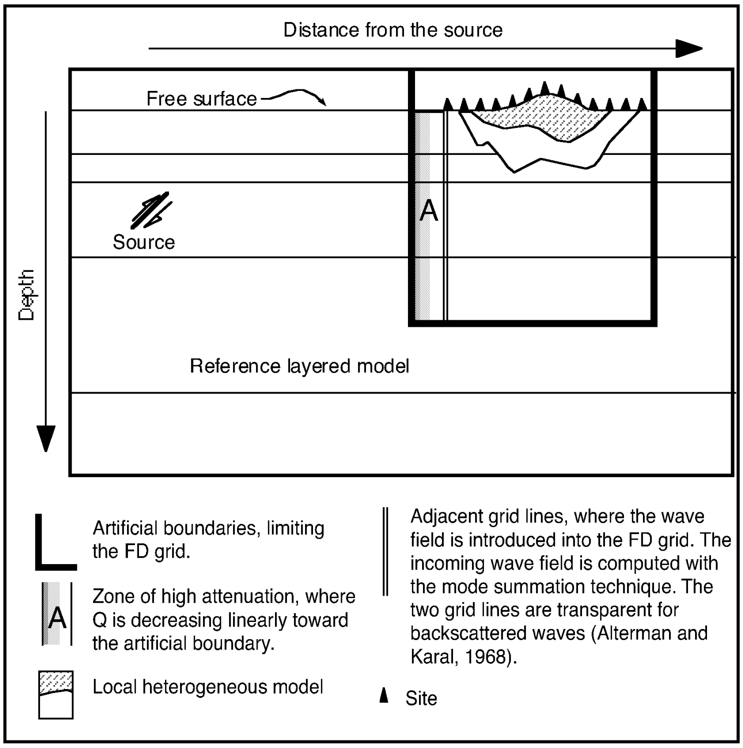




# Different source-section configurations

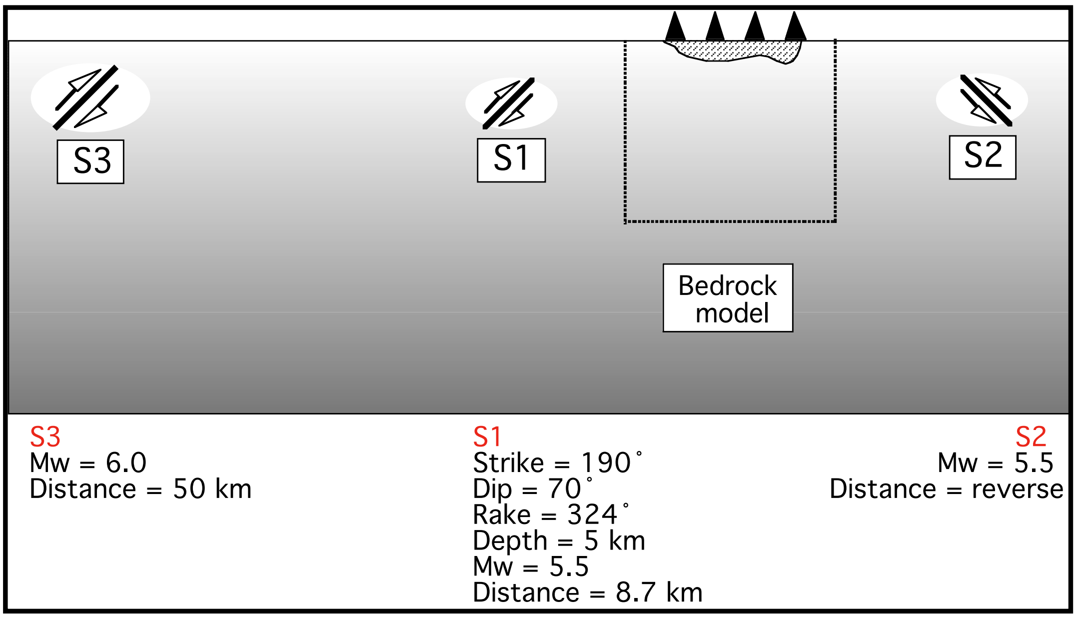

# Initial synthesis - radial

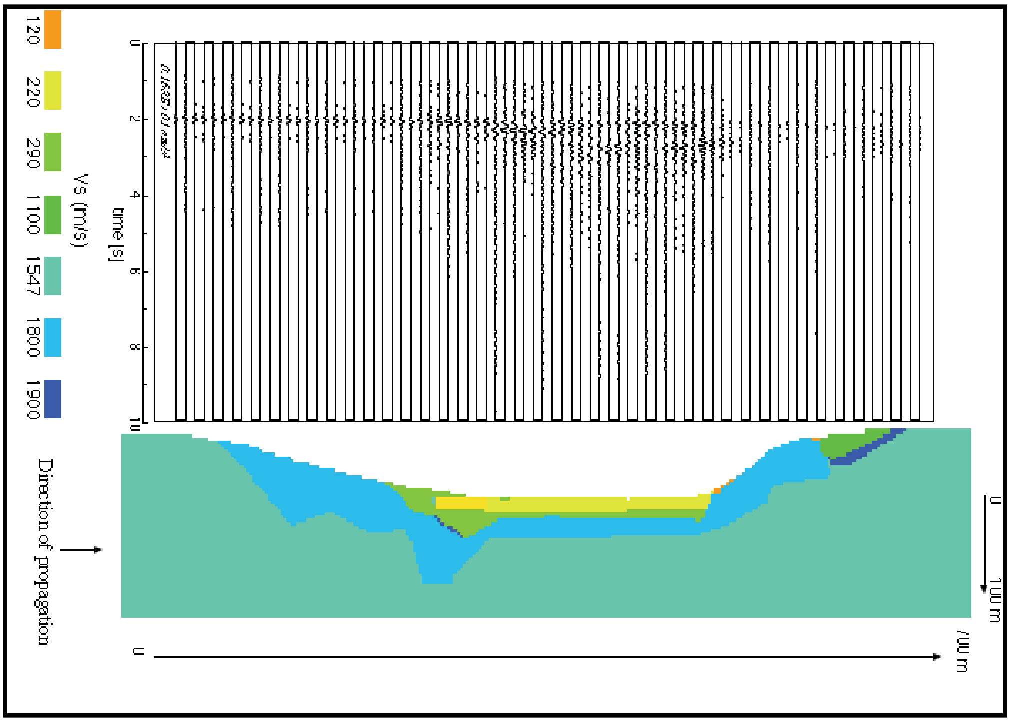


Definition of seismic input

# Synthetic accelerations and diffograms

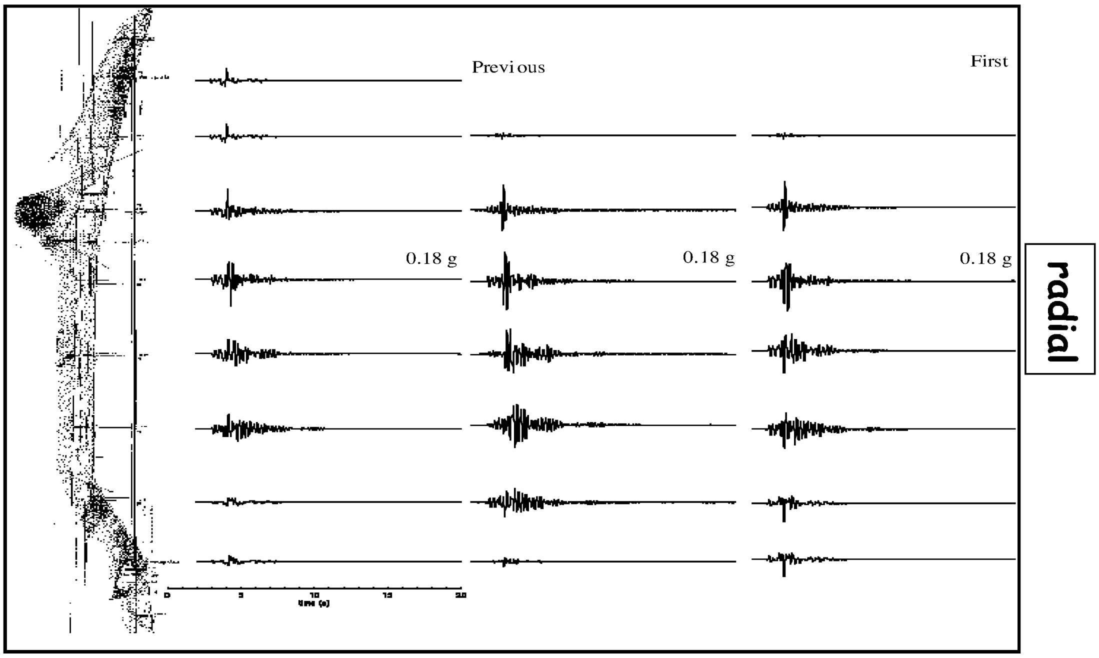


Definition of seismic input

# Synthetic accelerations and diffograms

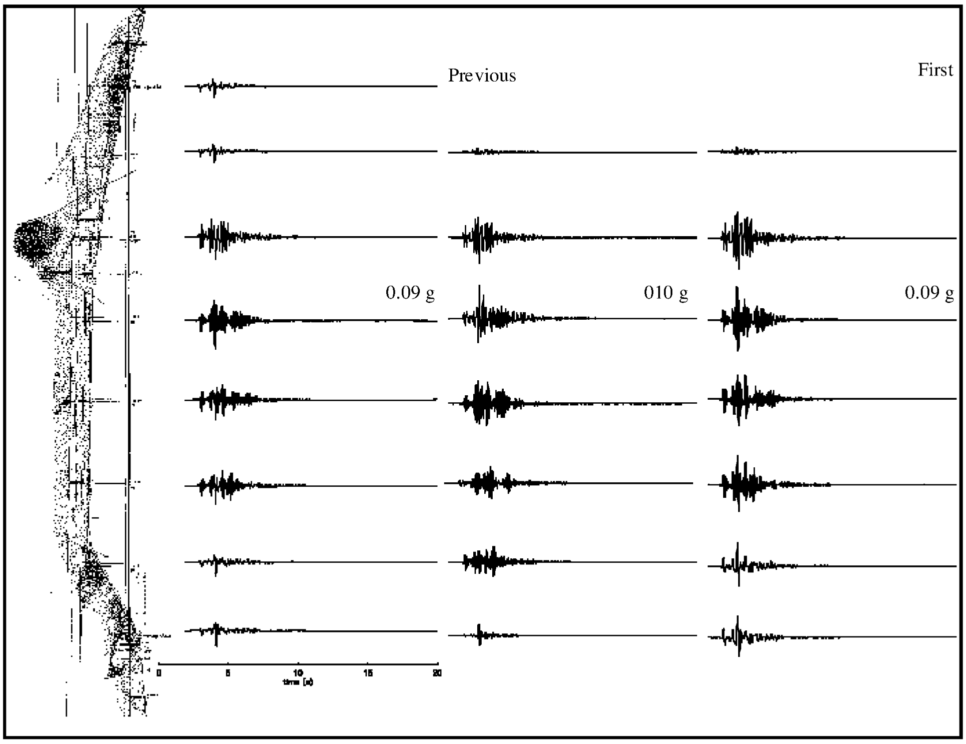


vertical

Definition of seismic input

# Synthetic accelerations and diffograms

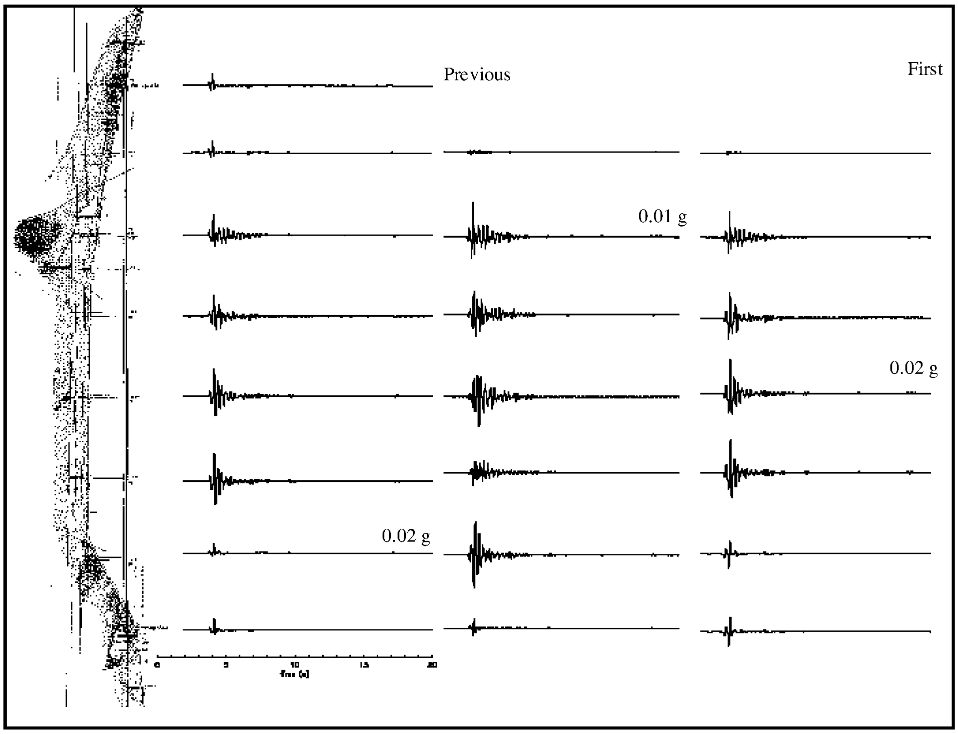


transverse

Case study examples

# Synthetic accelerations and diffograms

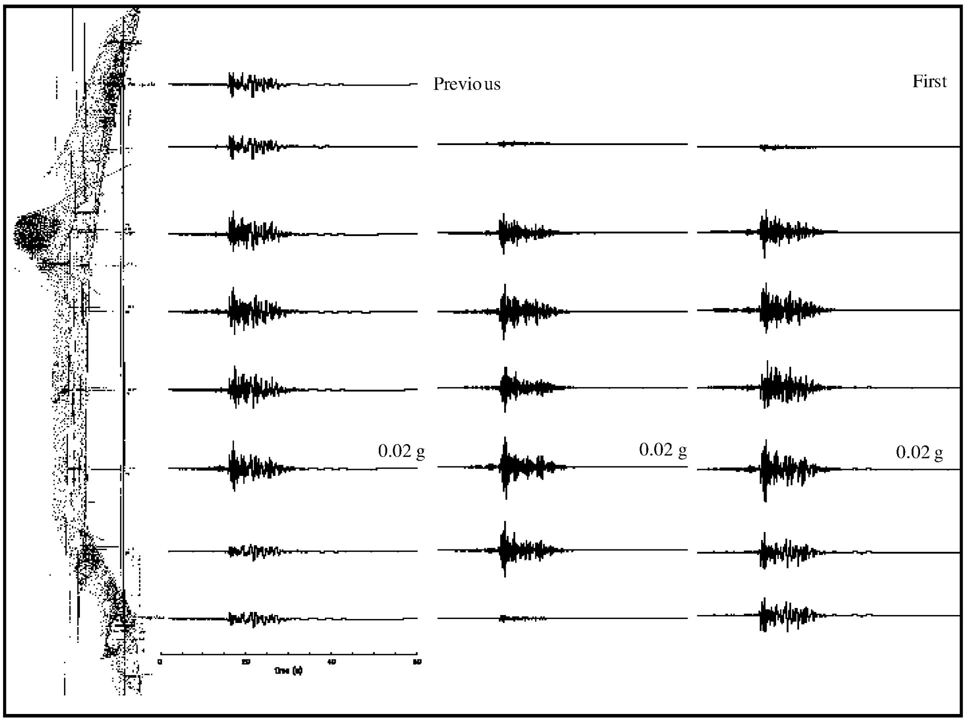


S3 - radial

Definition of seismic input

# LHM - Warth bridge - model

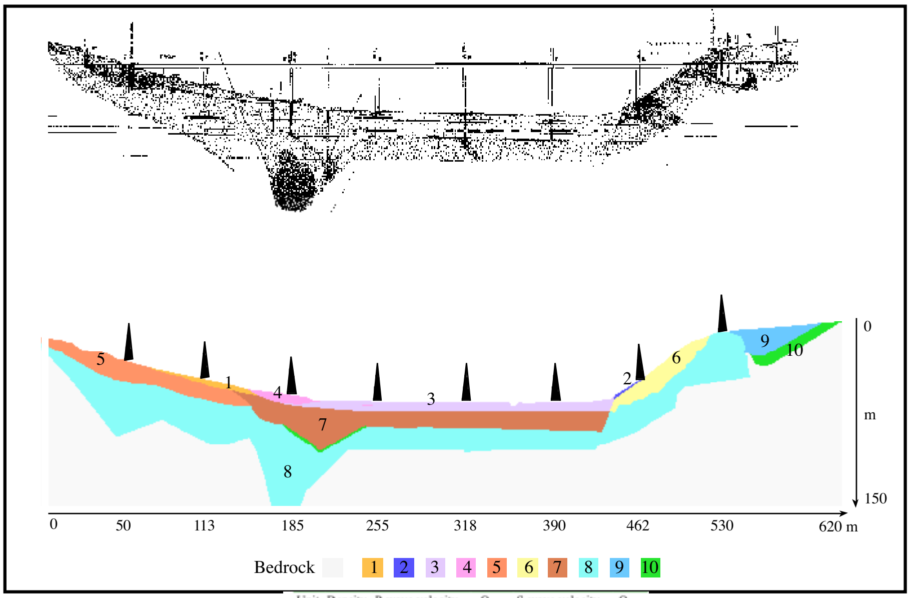


| Unit | Density g/cm³ | P-wave velocity km/s | $Q_P$ | S-wave velocity km/s | $Q_S$ |
|---|---|---|---|---|---|
| 1 | 1.5 | 0.30 | 40.0 | 0.20 | 15.0 |
| 2 | 1.7 | 0.49 | 40.0 | 0.25 | 15.0 |
| 3 | 2.0 | 0.70 | 50.0 | 0.26 | 20.0 |
| 4 | 1.8 | 0.70 | 50.0 | 0.29 | 20.0 |
| 5 | 2.3 | 0.80 | 50.0 | 0.30 | 20.0 |
| 6 | 2.3 | 0.80 | 50.0 | 0.40 | 20.0 |
| 7 | 1.8 | 1.70 | 50.0 | 0.50 | 20.0 |
| 8 | 2.3 | 2.10 | 150.0 | 1.00 | 60.0 |
| 9 | 2.3 | 3.00 | 150.0 | 1.90 | 60.0 |
| 10 | 2.2 | 1.80 | 100.0 | 1.10 | 40.0 |

# Synthetic accelerations and diffograms

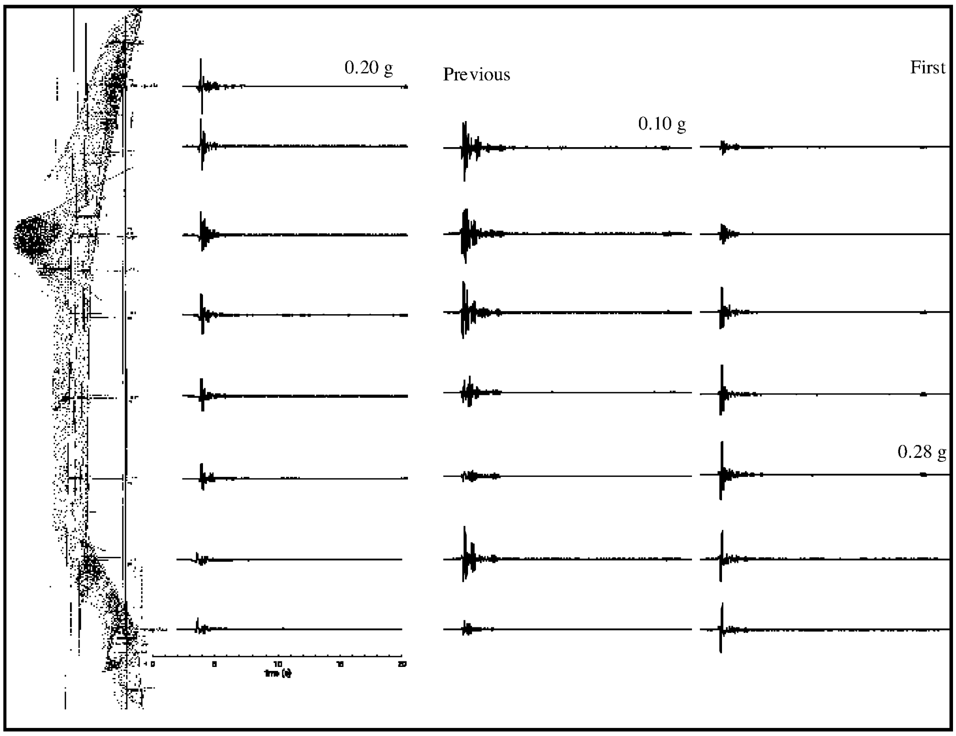


new - radial

Definition of seismic input

# Synthetic accelerations and diffograms
# Frequency domain - Amplitude spectra

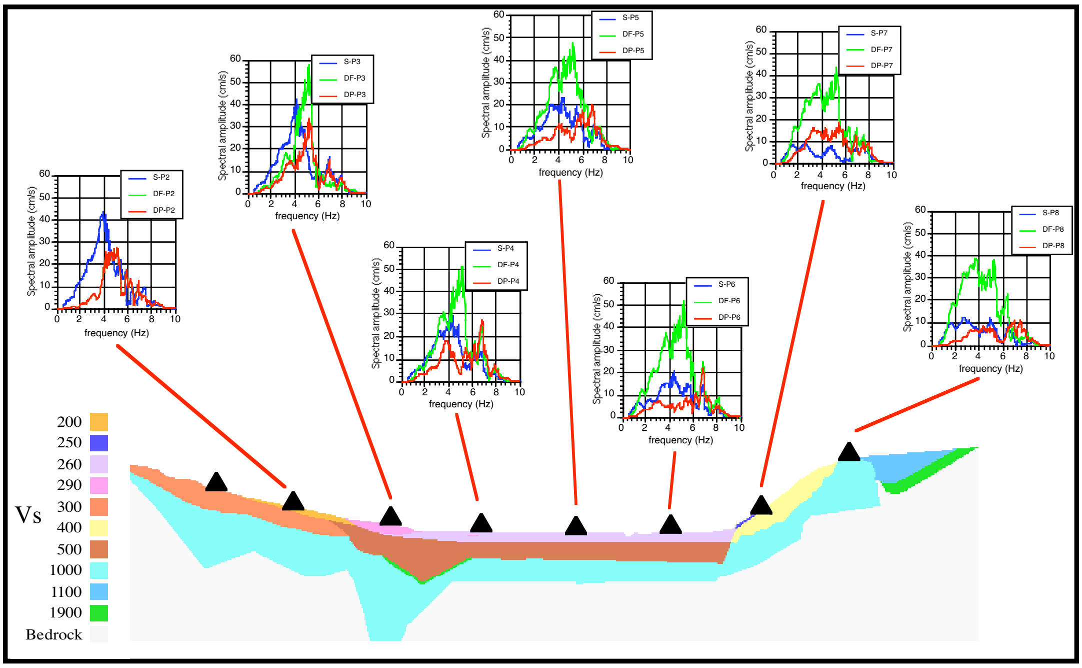


Seismic input-Fourier

# Synthetic accelerations and diffograms
# Frequency domain - Amplitude spectra

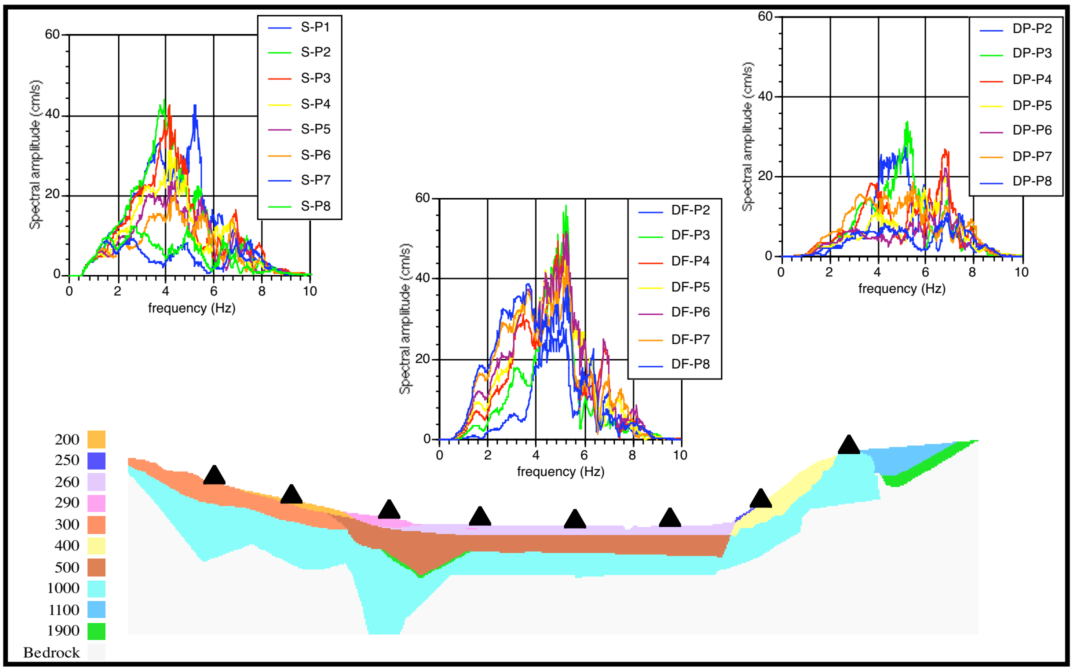


Seismic input-Fourier

# Synthetic accelerations
# RS domain - Amplification

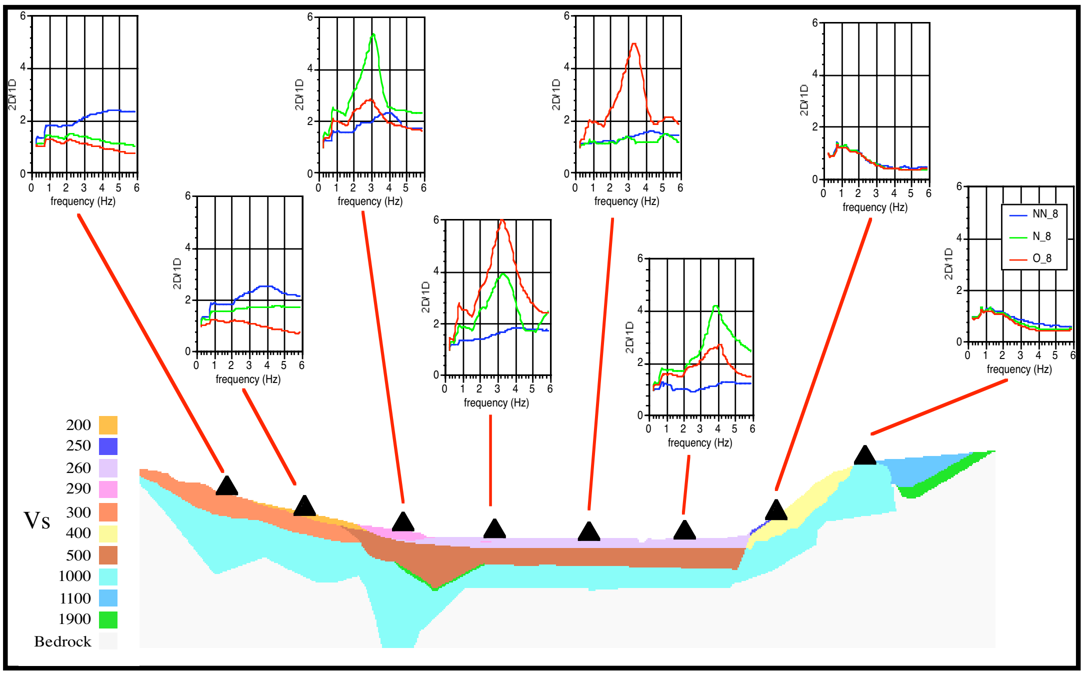


Seismic input-RSR

# PARAMETRIC STUDY - Fp towards MCE

All the focal mechanism parameters of the original source model have been varied in order to find the combination producing the maximum amplitude of the various ground motion components.

| Longitude (°) | Latitude (°) | Focal Depth (km) | Strike (°) | Dip (°) | Rake (°) | Magnitude Ms (Mb) |
|---|---|---|---|---|---|---|
| **16.120** | **47.730** | **18** | **190** | **70** | **324** | **5.5 (4.9)** |

1) Strike angle (Depth=5km)
2) Rake angle
3) Strike-Rake angles variation (Dip=45°)
4) Strike-Rake angles variation (Dip=70°)
5) Strike-Rake angles variation (Dip=90°)
6) Depth-Distance variation
(Strike=60°, Dip=70°,Rake=0, 90°)

The computations of synthetic seismograms (displacements, velocities and accelerations for the radial, transverse and vertical components) have been carried out with cut-off frequency 10 Hz.

# Parametric study 1: strike

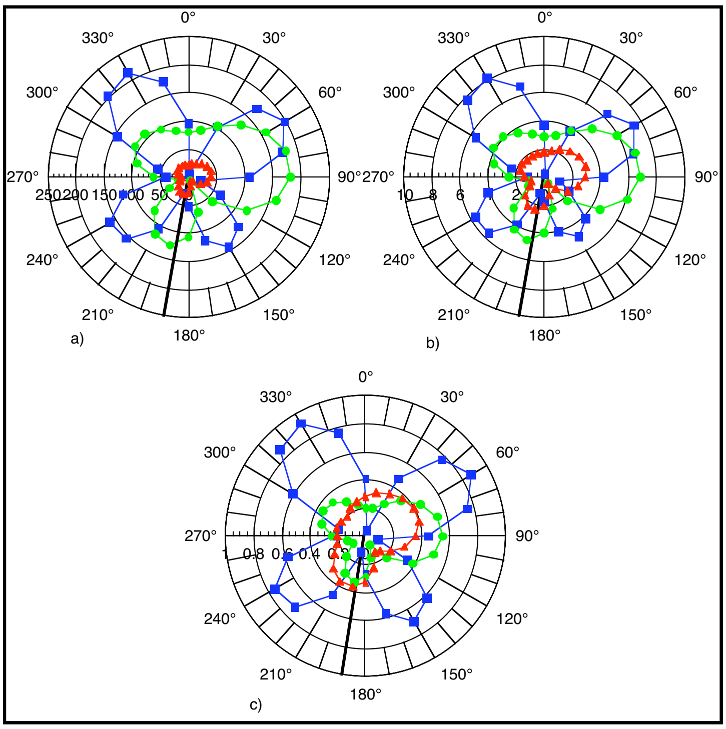


Polar plot of the maximum amplitude of the ground motion:
a) acceleration (cm/s$^2$)
b) velocity (cm/s)
c) displacement (cm)

versus the strike angle

for the three components:
transverse (squares);
radial (circles);
vertical (triangles)

# Parametric study 1: rake

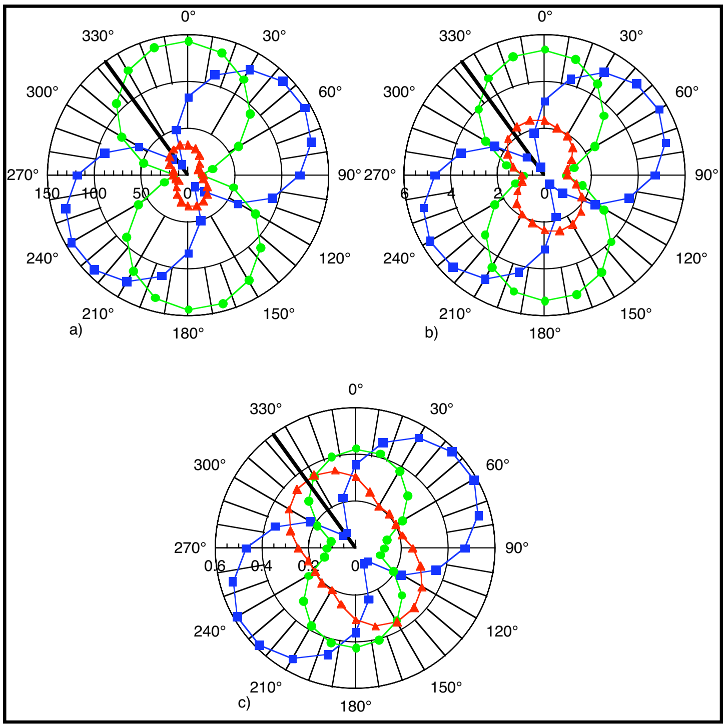


Polar plot of the maximum amplitude of the ground motion:
a) acceleration (cm/s$^2$)
b) velocity (cm/s)
c) displacement (cm)

versus the rake angle

for the three components:
transverse (squares);
radial (circles);
vertical (triangles)



# Parametric study 1: dip

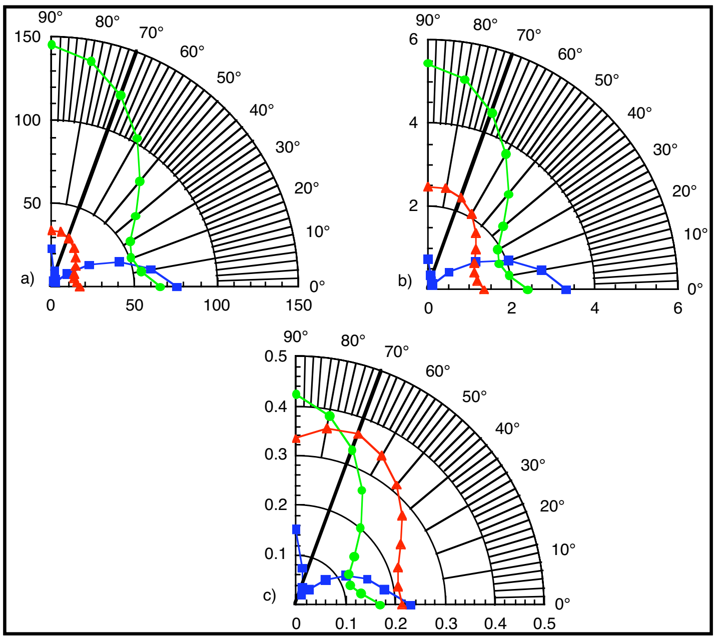


Polar plot of the maximum amplitude of the ground motion:
a) acceleration (cm/s$^2$)
b) velocity (cm/s);
c) displacement (cm)

versus the dip angle

for the three components:
transverse (squares);
radial (circles);
vertical (triangles)

# Parametric study 1: s&r

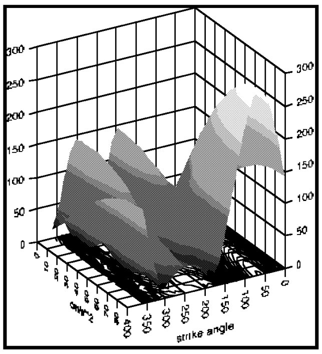


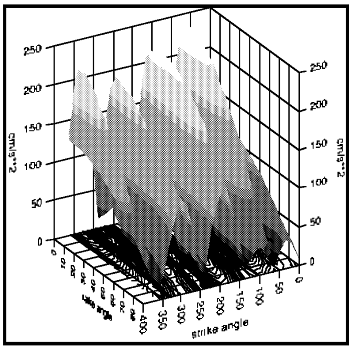


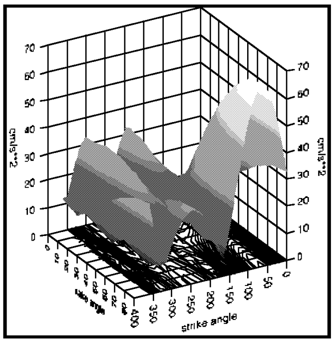


Polar plot of the maximum amplitude of the acceleration ground motion - dip angle is 70°

versus the strike and rake angle

for the three components of motion



# Parametric study 1: h&d

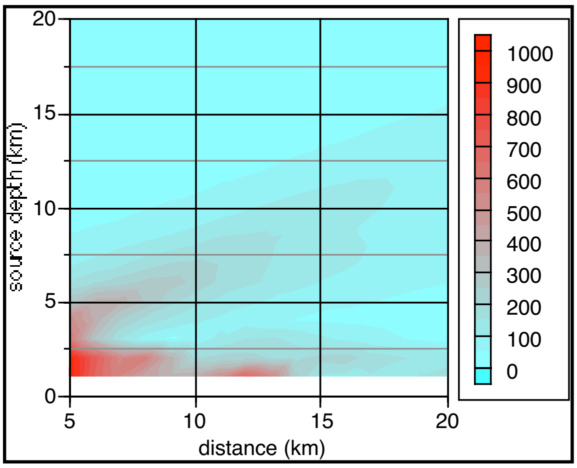


Plot of the maximum amplitude of the acceleration ground motion - cm/s$^2$ - versus the

epicentral distance
and
source depth

transverse component
dip angle=70°

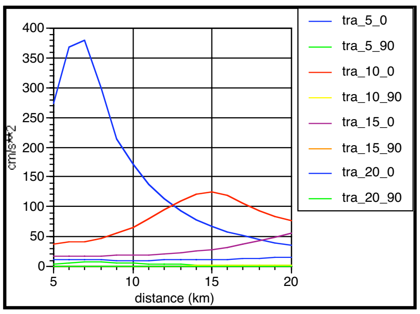

# Tranverse accelerograms M=5.5

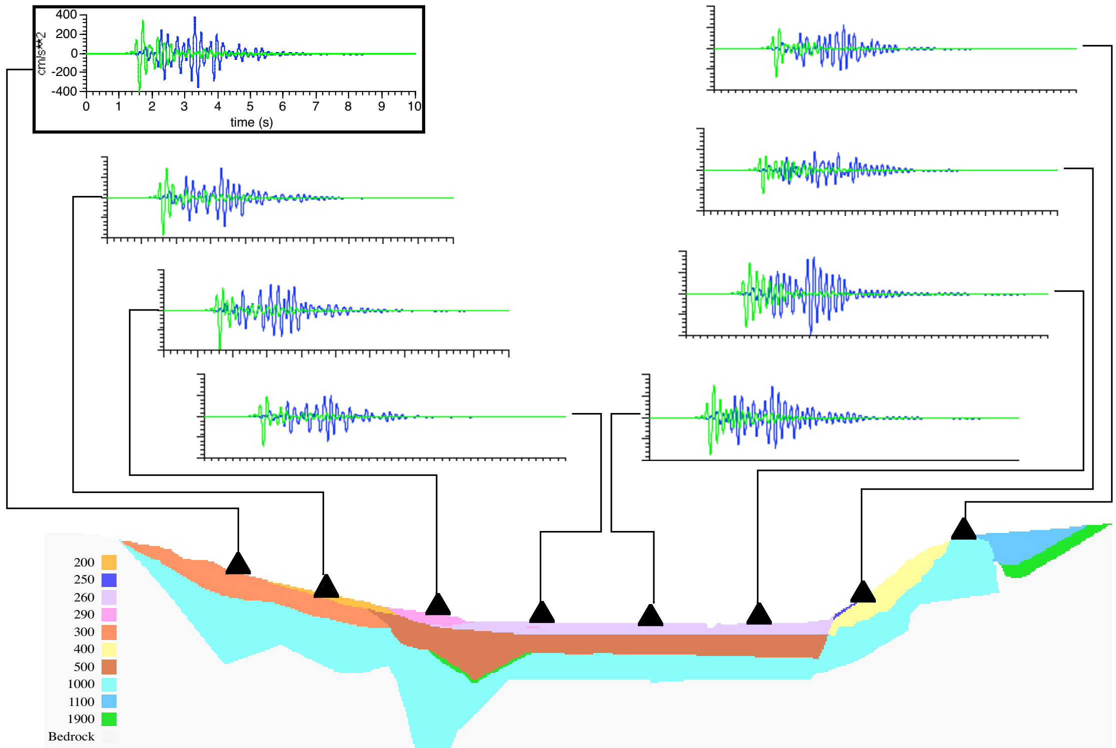




# Tranverse acceleration spectra

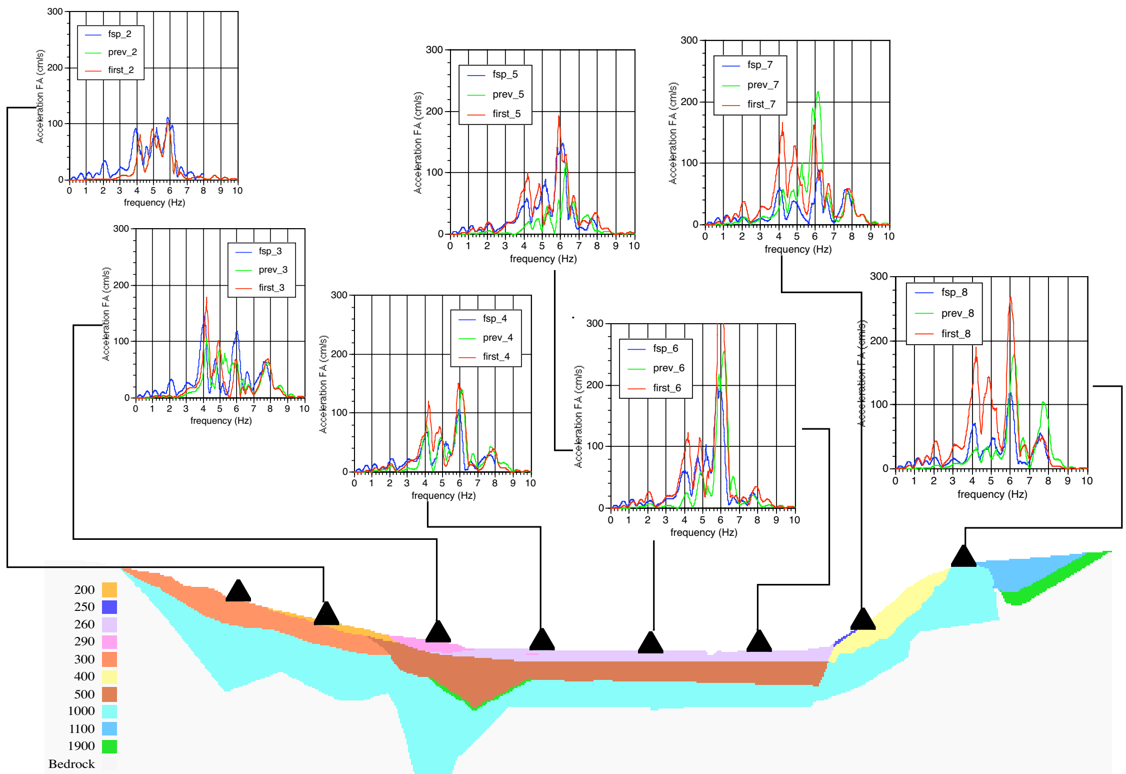

# PARAMETRIC STUDY 2 - Fp towards 1Hz

Another parametric study has been performed in order to find a seismic source-Warth site configuration providing a set of signals whose seismic energy is concentrated around 1 Hz, frequency that corresponds approximately to that of the fundamental transverse mode of oscillation of the bridge.

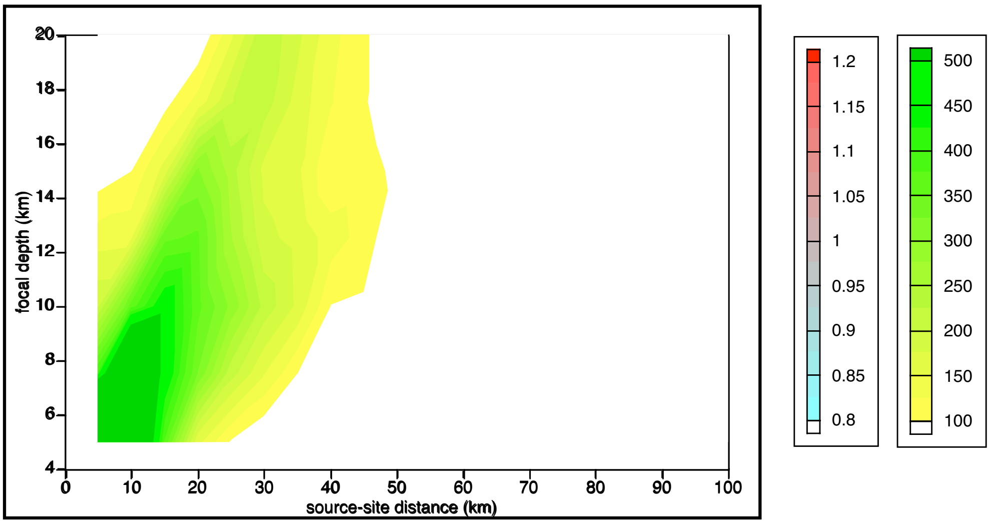


The results show that, in order to reach a relevant value of PGA (e.g. greater than 0.1g) in the desired period range (i.e. 0.8-1.2 s), an alternative and suitable configuration is a source
12 km deep at an epicentral distance of 30 km.

# Parametric study 2 - FS & RSR

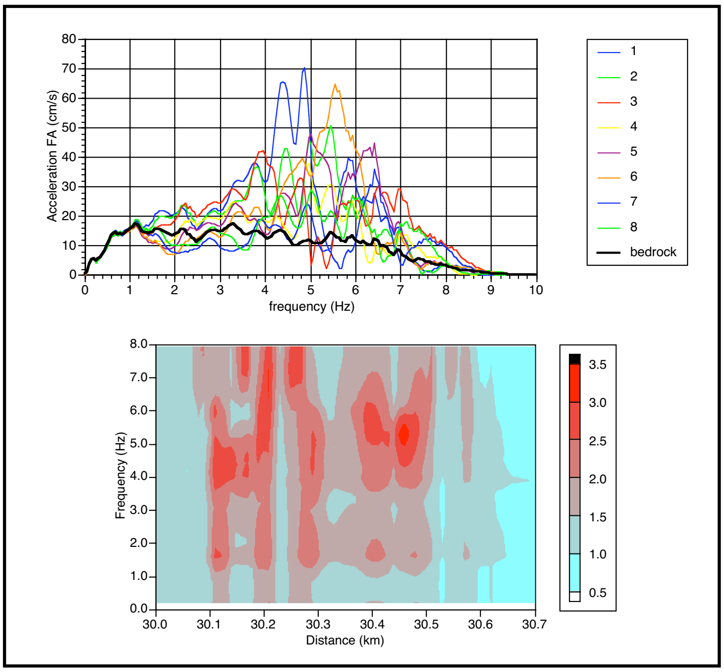


The results show that, the local structure beneath the Warth bridge greatly amplifies the frequency components between 3 and 7 Hz, i.e. a frequency range not corresponding to the fundamental transverse mode of oscillation of the bridge (about 0.8 Hz)

# Parametric study 3 - LMp towards 1Hz

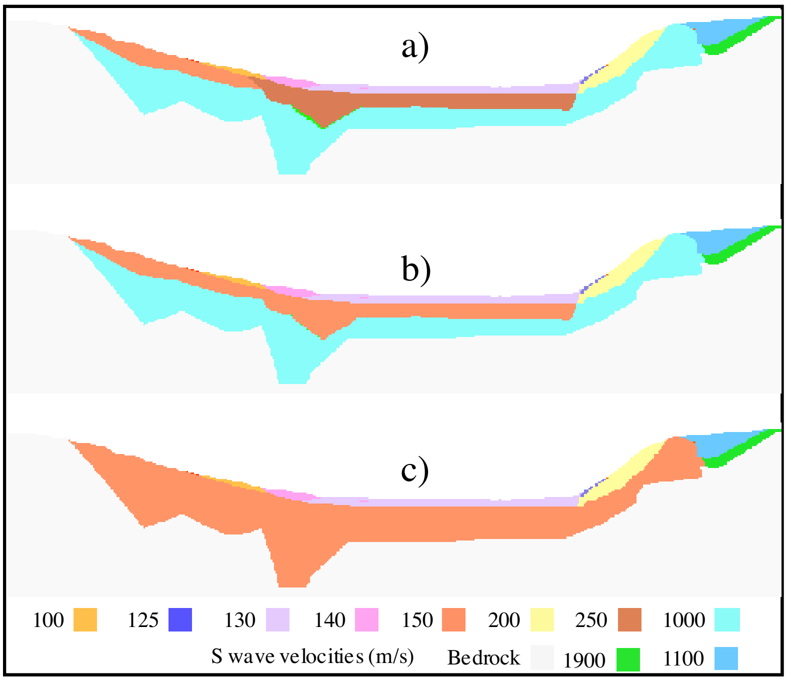


Local geotechnical models of Warth bridge section obtained lowering successively the S-wave velocities of the uppermost units



# Parametric study 3 FAS

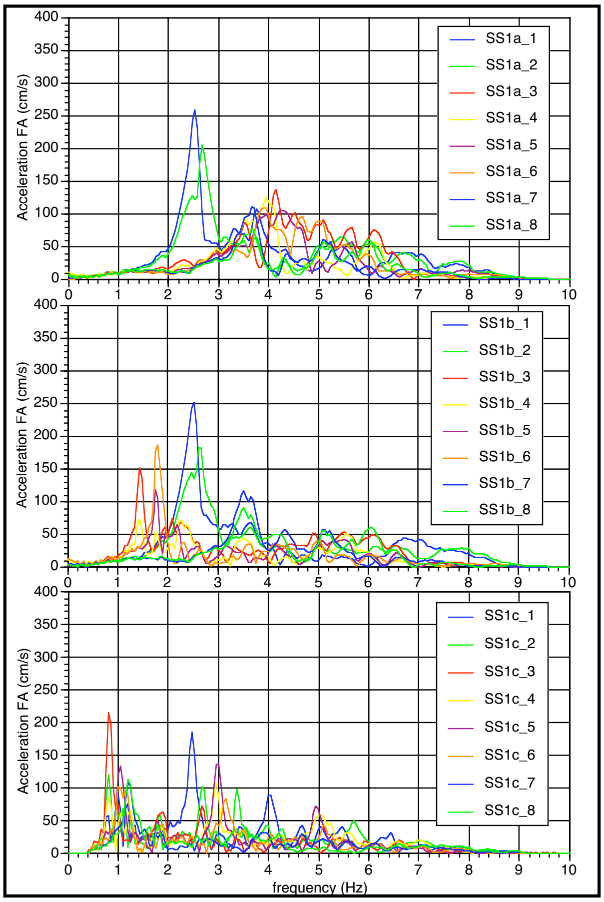


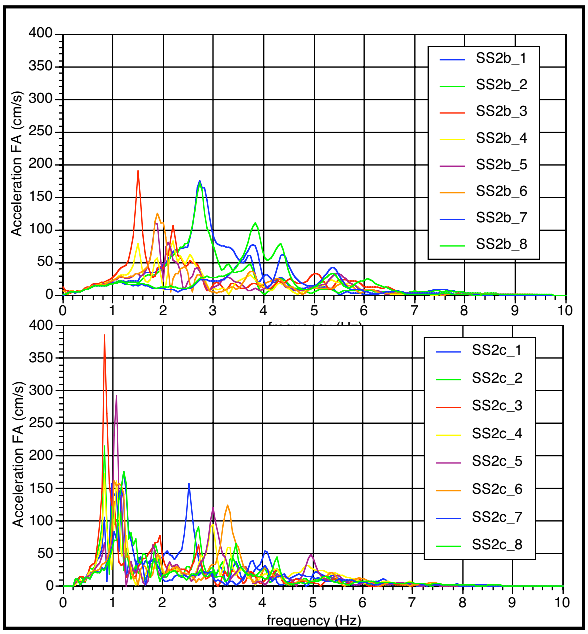

# Parametric study 3
# RSR

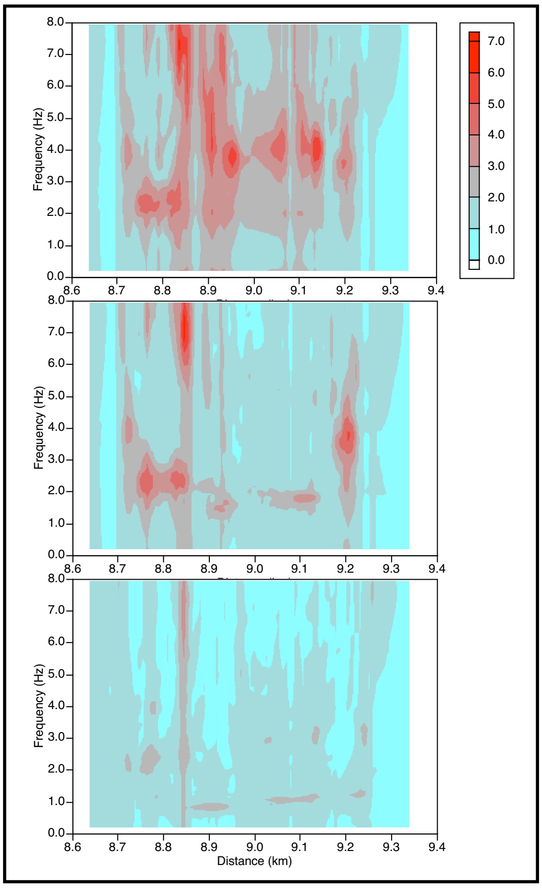


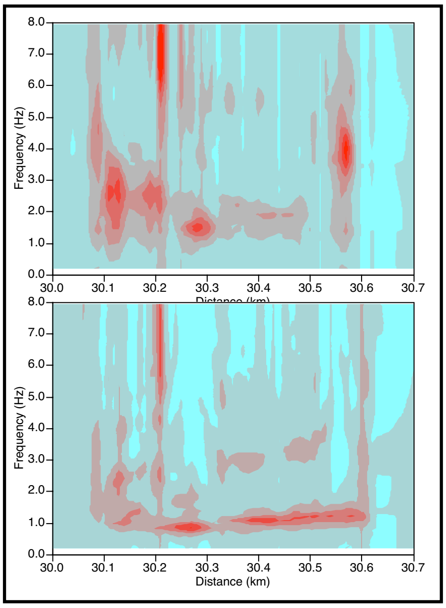


Case study examples

# Synthetic accelerations and diffograms

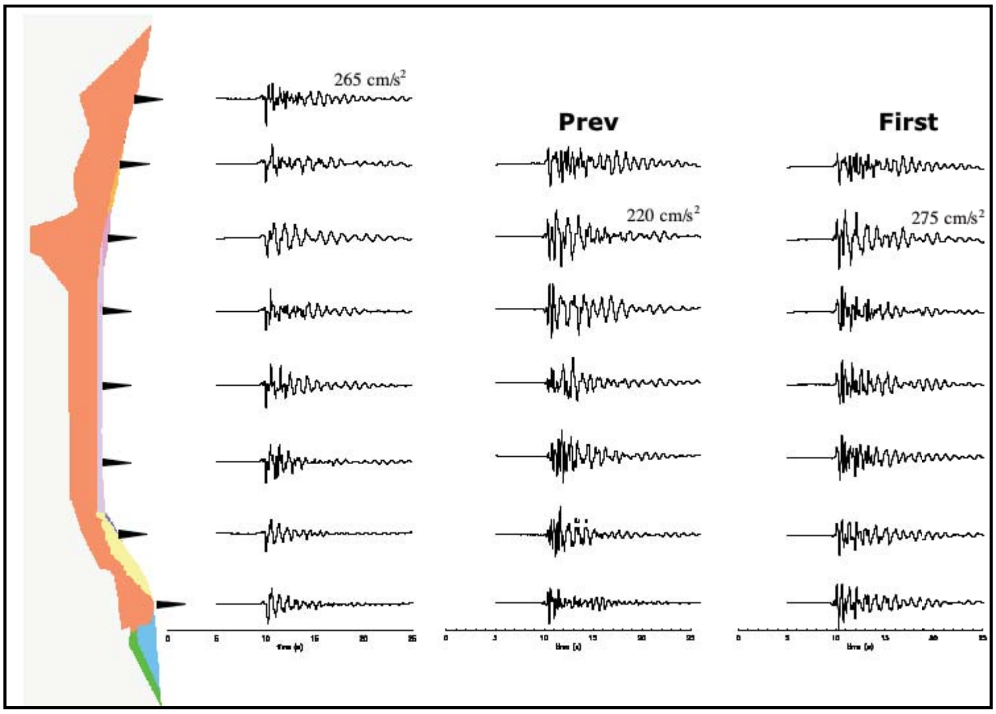


Case study examples

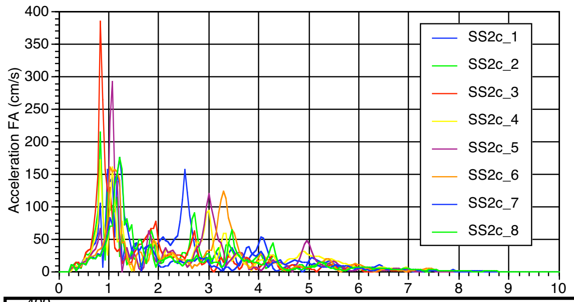


# Synthetic accelerations and diffograms FAS

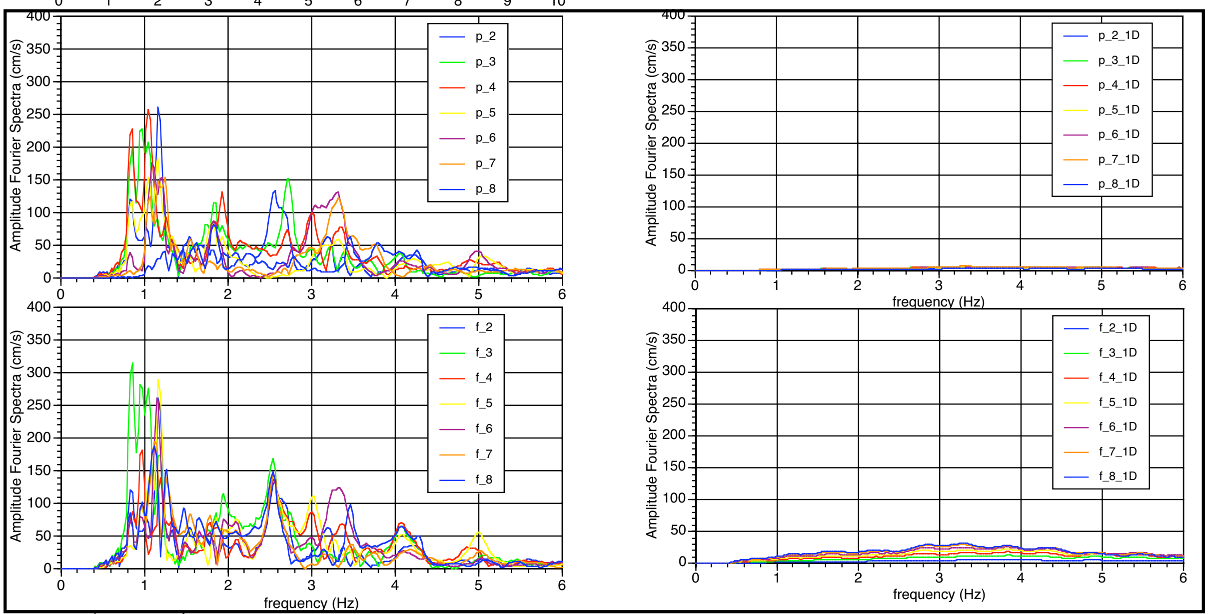


Case study examples

# Parametric study - ESp towards directivity

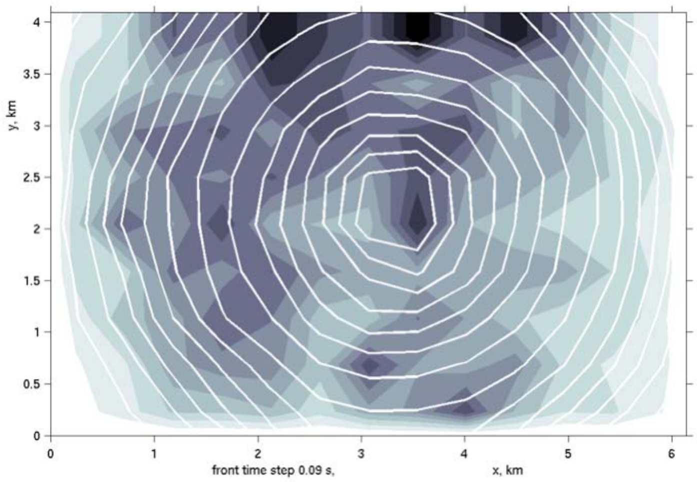


1st rupture model: bilateral at 3 positions

# Parametric study - ESp towards directivity

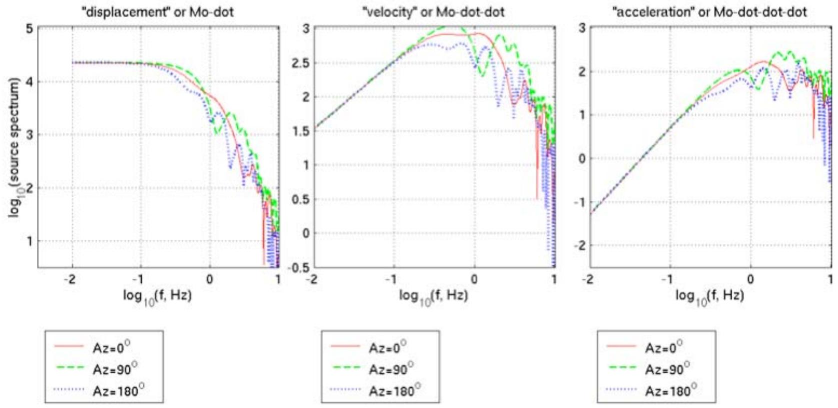


1st rupture model: bilateral at 3 positions

# Parametric study - ESp towards directivity

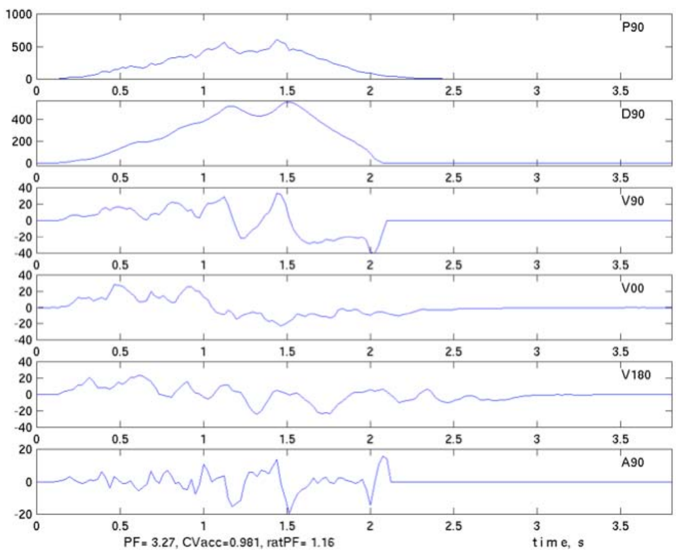


1st rupture model: bilateral at 3 positions

## Parametric study - ESp towards directivity

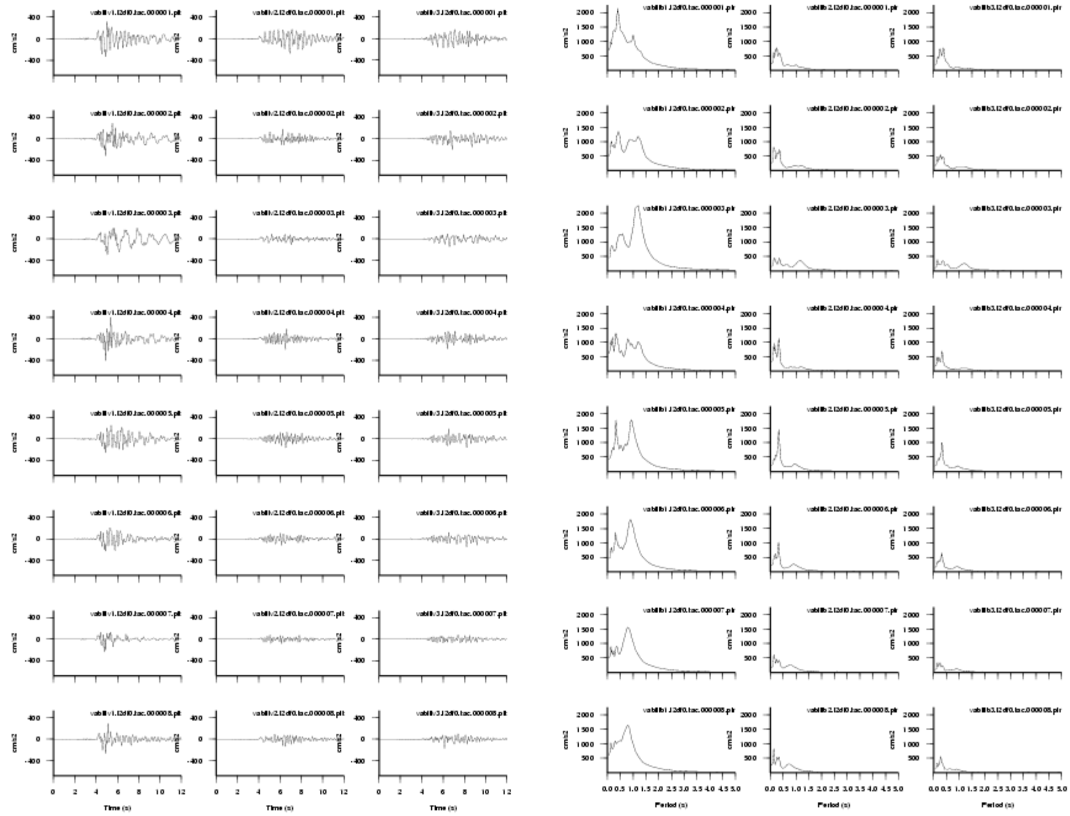

1st rupture model: bilateral at 3 positions

## Parametric study - ESp towards directivity

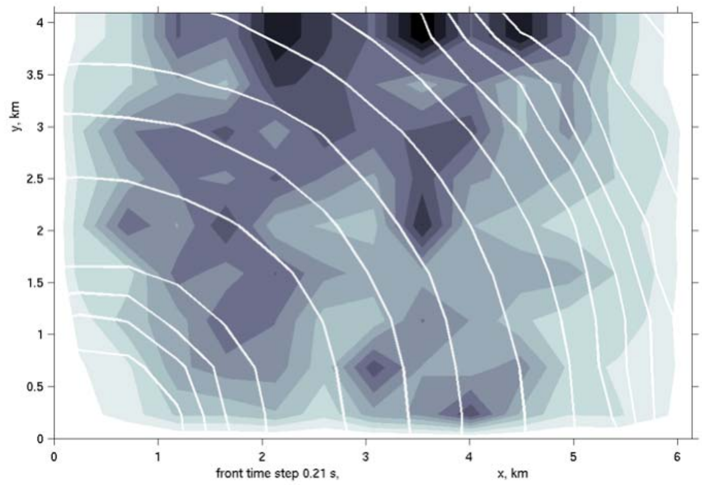


Case study examples

2nd rupture model: unilateral at 3 positions

# Parametric study - ESp towards directivity

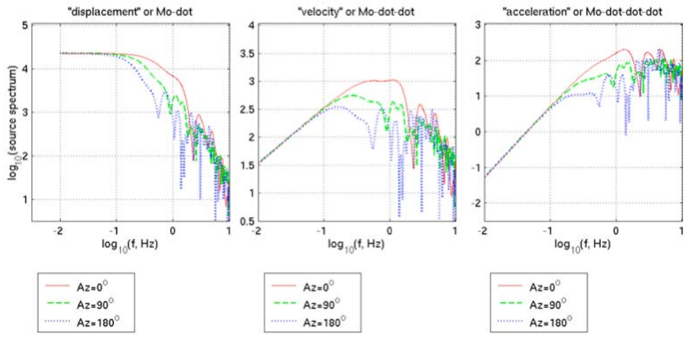


Case study examples

2nd rupture model: unilateral at 3 positions

# Parametric study - ESp towards directivity

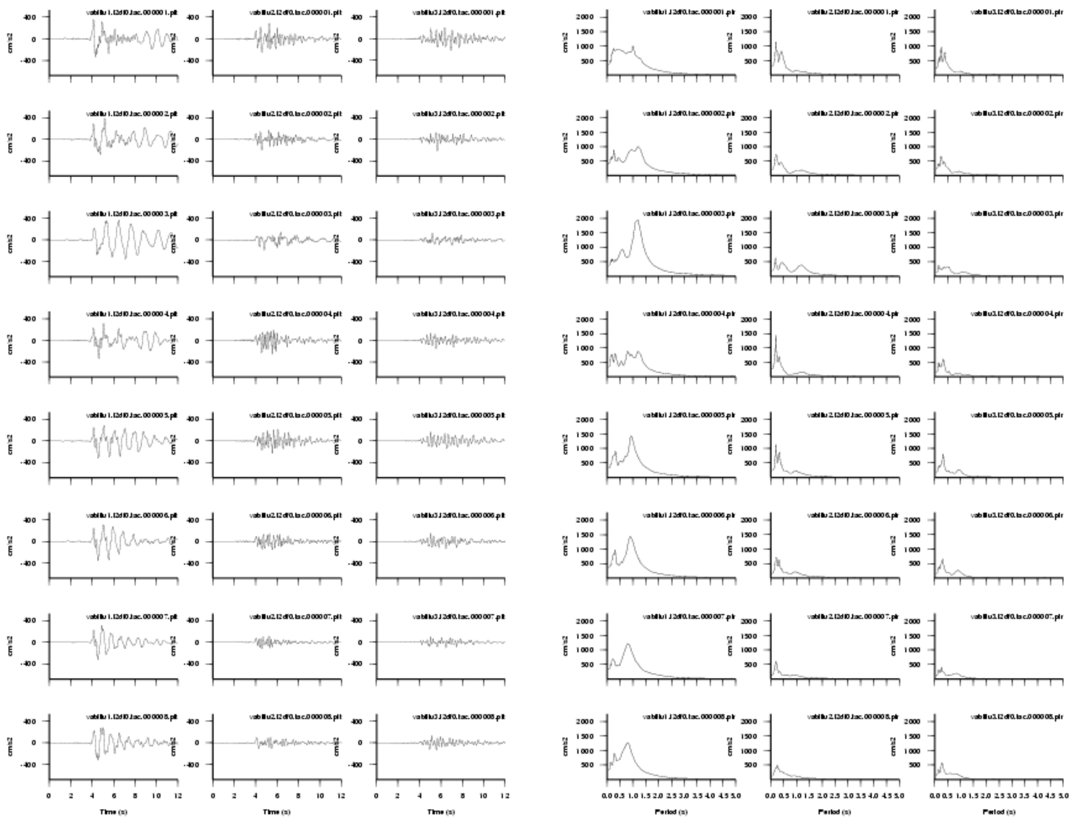


Case study examples

2nd rupture model: unilateral at 3 positions

# Parametric study - ESp towards directivity

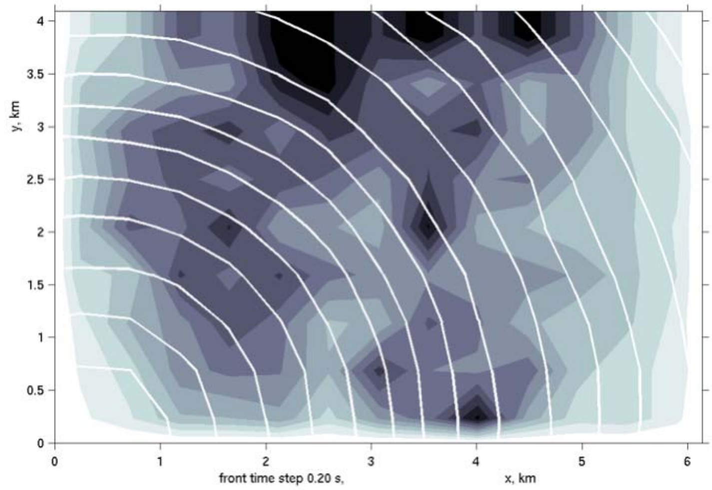


Case study examples

3rd rupture model: different $v_r$ at 3 positions

# Parametric study - ESp towards directivity

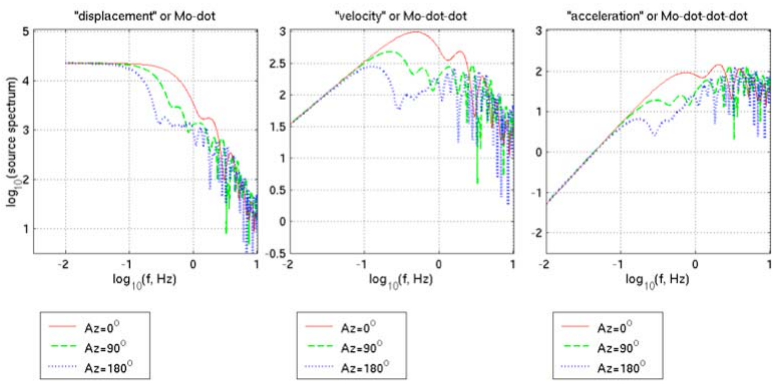


Case study examples

3rd rupture model: different $v_r$ at 3 positions

# Parametric study - ESp towards directivity

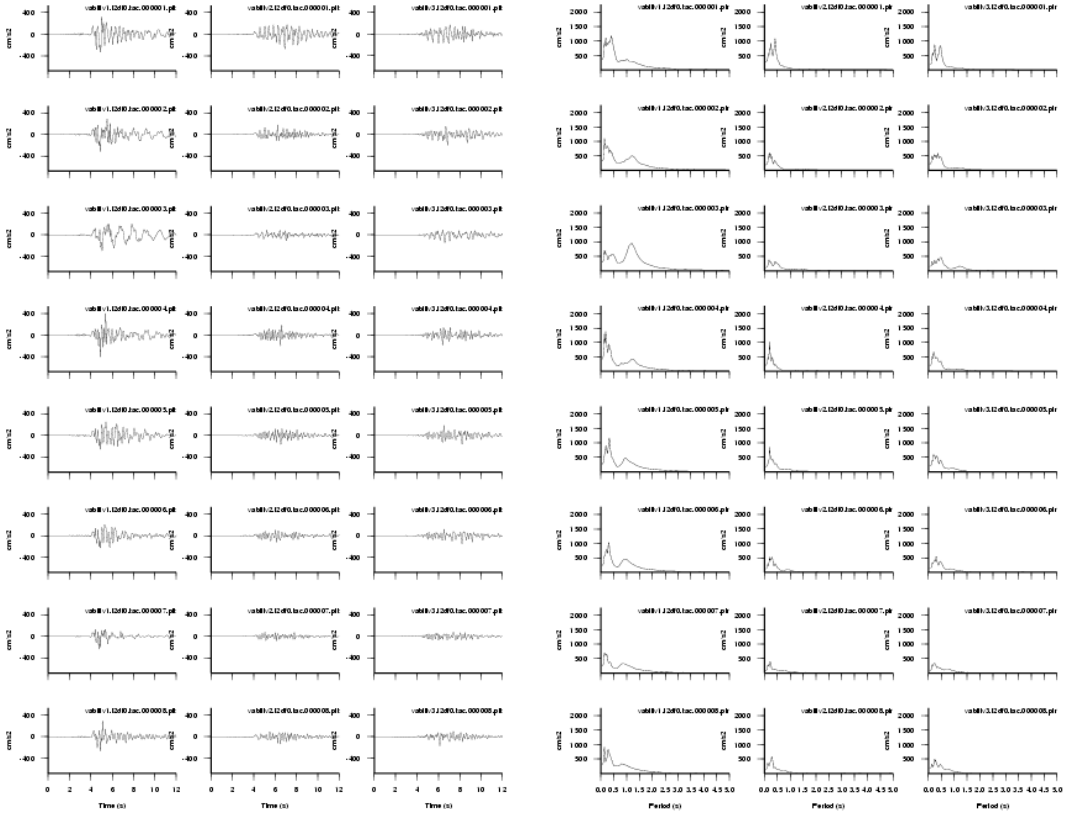


Case study examples

3rd rupture model: different $v_r$ at 3 positions

# Parametric study 4 - ESp towards directivity

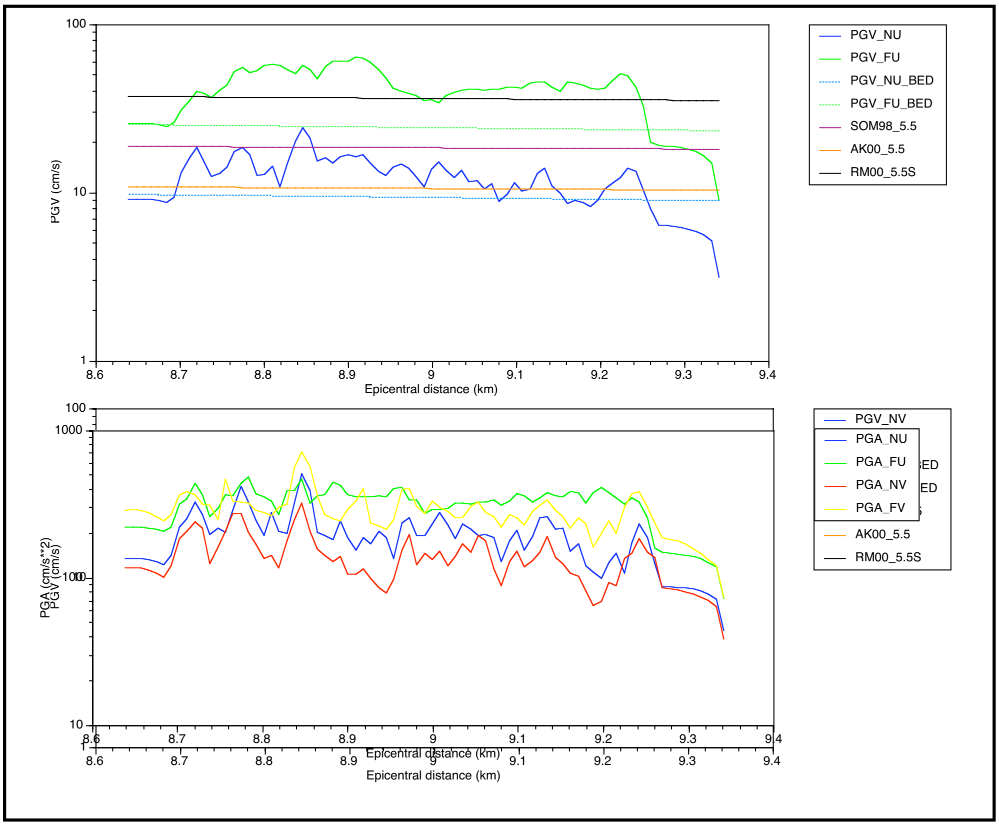


Parametric study 4 - ES

PGV - PGA

# Parametric study 4 - ESp towards directivity

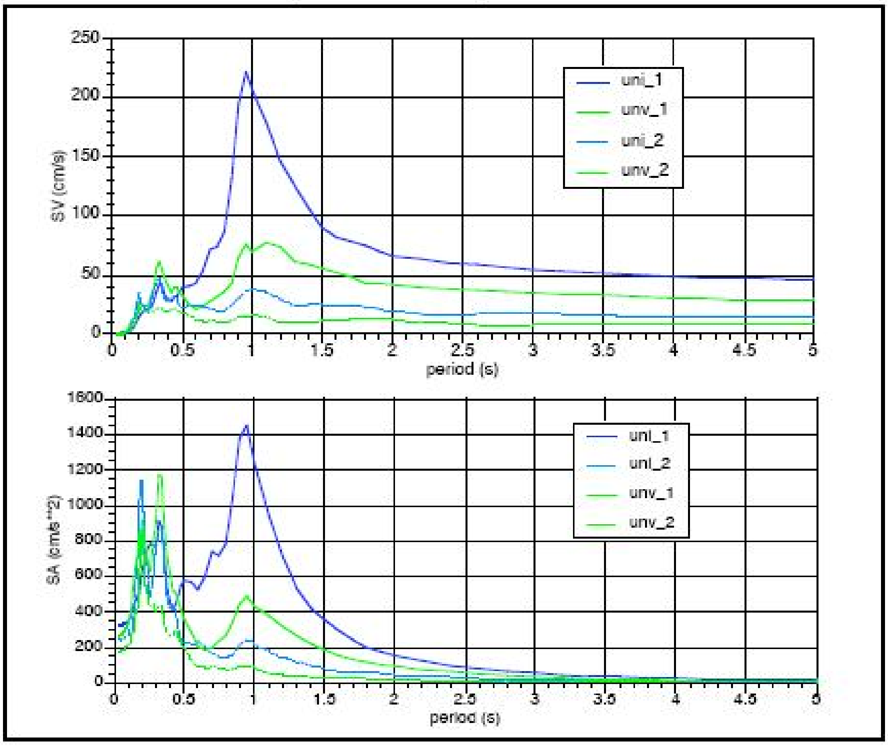


Parametric study 4 - ES

response spectra

# Implementation of PSD tests

Joint Research Centre

## PSD WITH SUBSTRUCTURING

### Application to the Warth Bridge, Austria

Construction of the large-scale bridge piers outside of the ELSA lab

Physical piers A40 & A70 in the lab

Numerical models for the substructured piers A20, A30

Numerical models for the substructured piers A50, A60

Numerical model for the deck and PSD master

Master experimental process

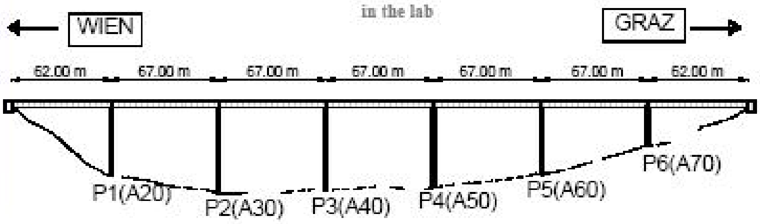


Warth Bridge

elsa

# Implementation of PSD tests

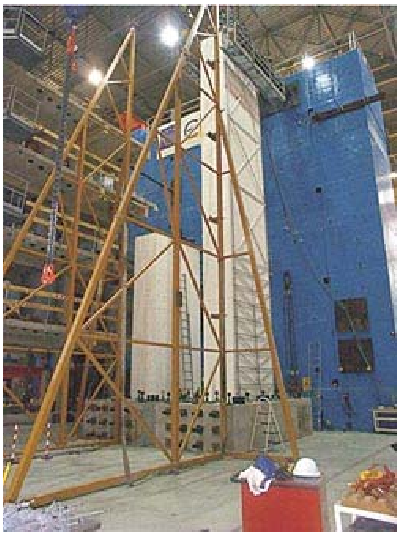

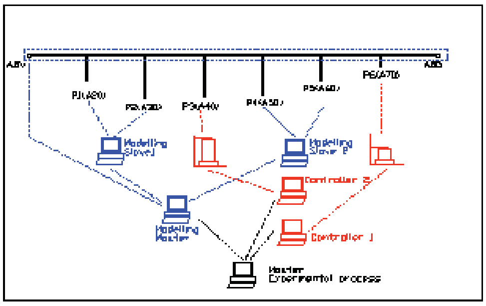

(a) physical piers in the lab, (b), schematic representation
(c) workstations running the PSD algorithm and controlling the test



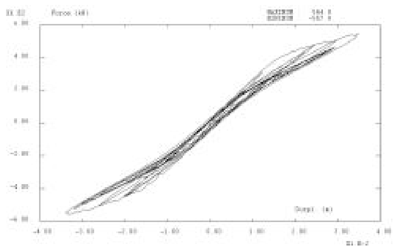

Force-displacement for Low-level earthquake - experimental results Pier A40

Identification of insufficient seismic detailing. tall pier A40, buckling of longitudinal reinforcement at h = 3.5m

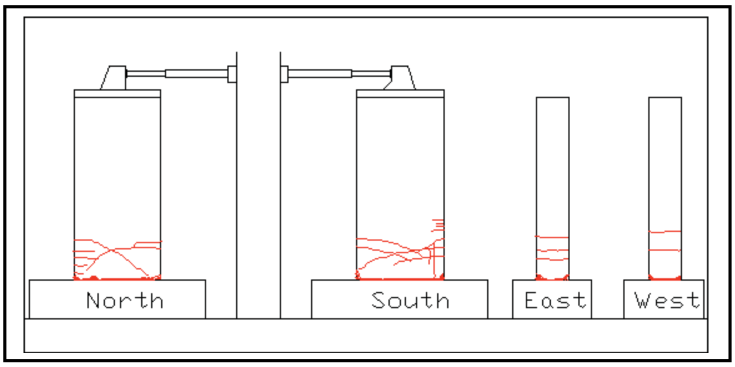


Damage pattern after the end of the High-Level Earthquake PSD test, short pier A70.

# Conclusions - 1

- Different ground motions at the Warth site have been studied in order to define the maximum excitation in longitudinal and transverse direction, which are consistent both with the Maximum Credible Earthquake and with the Maximum Design.
- The main practical conclusion of our analysis, verified by laboratory experiments carried out at JRC-ISPRA, is that the Warth bridge is likely to well stand the most severe seismic input compatible with the seismic regime of the Eastern Alps.
- With the parametric study we have defined a seismic source-Warth site configuration that provides a set of signals whose seismic energy is concentrated around 1 Hz, frequency that corresponds approximately to that of the fundamental transverse mode of oscillation of the bridge.



# Conclusions - 2

- The results show that lateral heterogeneity can produce strong spatial variations in the ground motion even at small incremental distances.
- Such variations can hardly be accounted for by the stochastic models commonly used in engineering practice.
- In absolute terms, the differential motion amplitude is comparable with the input motion amplitude when displacement, velocity and acceleration domains are considered.
- On the base of the existing empirical regression relations between Intensity and peak values of ground motion a general result of our modeling is that the effect of the differential motion can cause an increment greater than one unit in the seismic intensity experienced by the bridge, with respect to the average intensity affecting the area where the bridge is built.

# References


Panza, G.F., Romanelli, F. and Vaccari, F. (2001). "Seismic wave propagation in laterally heterogeneous anelastic media: theory and applications to the seismic zonation", **Advances in Geophysics**, Academic press, 43, 1-95.

Romanelli, F., Vaccari, F. and Panza, G.F. (2003). "Realistic modelling of the effects of asynchronous motion at the base of bridge piers", **Journal of Seismology and Earthquake Engineering**, Vol. 6, No. 2, pp. 17-26.

Romanelli, F., Vaccari, F. and Panza, G.F. (2003). "Realistic Modelling of the Seismic Input: Site Effects and Parametric Studies", **Journal of Seismology and Earthquake Engineering**, Vol. 5, No. 3, pp. 27-39.